BS ISO 26872:2010

BSI Standards Publication

# Space systems — Disposal of satellites operating at geosynchronous altitude



*raising standards worldwide*™

**National foreword**

This British Standard is the UK implementation of ISO 26872:2010.

The UK participation in its preparation was entrusted to Technical Committee ACE/68/-/3, Space systems and operations - Operations and Ground Support.

A list of organizations represented on this committee can be obtained on request to its secretary.

This publication does not purport to include all the necessary provisions of a contract. Users are responsible for its correct application.



ISBN 978 0 580 57841 0

ICS 49.140

**Compliance with a British Standard cannot confer immunity from legal obligations.**

This British Standard was published under the authority of the Standards Policy and Strategy Committee on 31 October 2010.

**Amendments issued since publication**

| Date | Text affected |
|---|---|

BS ISO 26872:2010

INTERNATIONAL STANDARD

**ISO 26872**

First edition
2010-09-15

# Space systems — Disposal of satellites operating at geosynchronous altitude

*Systèmes spatiaux — Élimination des satellites opérant à une altitude géostionnaire*

Reference number
ISO 26872:2010(E)



ISO copyright office
Case postale 56 • CH-1211 Geneva 20
Tel. + 41 22 749 01 11
Fax + 41 22 749 09 47
E-mail copyright@iso.org
Web www.iso.org

Published in Switzerland

# Contents

Page

# Foreword

ISO (the International Organization for Standardization) is a worldwide federation of national standards bodies (ISO member bodies). The work of preparing International Standards is normally carried out through ISO technical committees. Each member body interested in a subject for which a technical committee has been established has the right to be represented on that committee. International organizations, governmental and non-governmental, in liaison with ISO, also take part in the work. ISO collaborates closely with the International Electrotechnical Commission (IEC) on all matters of electrotechnical standardization.

International Standards are drafted in accordance with the rules given in the ISO/IEC Directives, Part 2.

The main task of technical committees is to prepare International Standards. Draft International Standards adopted by the technical committees are circulated to the member bodies for voting. Publication as an International Standard requires approval by at least 75 % of the member bodies casting a vote.

Attention is drawn to the possibility that some of the elements of this document may be the subject of patent rights. ISO shall not be held responsible for identifying any or all such patent rights.

ISO 26872 was prepared by Technical Committee ISO/TC 20, *Aircraft and space vehicles*, Subcommittee SC 14, *Space systems and operations*.

# Introduction

This International Standard prescribes requirements for planning and executing manoeuvres and operations to remove an operating satellite from geosynchronous orbit at the end of its mission and place it in an orbit for final disposal where it will not pose a future hazard to satellites operating in the geosynchronous ring.

This International Standard includes requirements related to the following:

— when the disposal action needs to be initiated,

— selecting the final disposal orbit,

— executing the disposal action successfully, and

— depleting all energy sources to prevent explosions after disposal.

End-of-mission disposal of an Earth-orbiting satellite broadly means the following:

a) removing the satellite from the region of space where other satellites are operating, so as not to interfere or collide with these other users of space in the future, and

b) ensuring that the disposed object is left in an inert state and is incapable of generating an explosive event that could release debris which might threaten operating satellites[1)].

For satellites operating in the geosynchronous belt, the most effective means of disposal is first to re-orbit the satellite to a super-synchronous orbit above the region of operating spacecraft and the manoeuvre corridor used for relocating operating satellites to new longitudinal slots, and then to discharge batteries and vent propellants and take other actions to preclude a debris-producing event.

1) Further information will be provided in the future International Standard, ISO 16127.

INTERNATIONAL STANDARD ISO 26872:2010(E)

# Space systems — Disposal of satellites operating at geosynchronous altitude

**IMPORTANT — The electronic file of this document contains colours which are considered to be useful for the correct understanding of the document. Users should therefore consider printing this document using a colour printer.**

## 1 Scope

This International Standard specifies requirements for the following:

— planning for disposal of satellites operating at geosynchronous altitude to ensure that final disposal is sufficiently characterized and that adequate propellant will be reserved for the manoeuvre;

— selecting final disposal orbits where the satellite will not re-enter the operational region within the next 100 years;

— executing the disposal manoeuvre successfully;

— depleting all energy sources on board the vehicle before the end of its life to minimize the possibility of an event that can produce debris.

This International Standard provides techniques for planning and executing the disposal of space hardware that reflect current internationally accepted guidelines and consider current operational procedures and best practices.

## 2 Normative references

The following referenced documents are indispensable for the application of this document. For dated references, only the edition cited applies. For undated references, the latest edition of the referenced document (including any amendments) applies.

ISO 24113:2010, *Space systems — Space debris mitigation requirements*

## 3 Terms and definitions

For the purposes of this document, the terms and definitions given in ISO 24113 and the following apply.

**3.1**
**inclination excursion region**
region in space occupied either by a non-operational geostationary satellite or by an operational geosynchronous satellite without inclination station-keeping

**3.2**
**re-orbit manoeuvre**
action of moving a satellite to a new orbit

**3.3**
**satellite**
manufactured object or vehicle intended to orbit the earth, the moon or another celestial body

# 4 Symbols and abbreviated terms

## 4.1 Symbols

| | |
|---|---|
| $a$ | semi-major axis |
| $C_R$ | solar radiation pressure coefficient of the spacecraft[2] ($0 < C_R < 2$) |
| $e$ | eccentricity |
| $h_p$ | perigee altitude |
| $i$ | inclination |
| $I_{sp}$ | specific impulse |
| $L_S$ | solar longitude |
| $M$ | mean anomaly |
| $p$ | semilatus rectum or semi-parameter [$p = a(1 - e^2)$] |
| $r$ | radius of orbit |
| $v$ | true anomaly |
| $\mu$ | Earth gravitational constant |
| $\sigma$ | standard deviation or the positive root of the variance, which measures the dispersion of the data |
| $\Omega$ | right ascension of ascending node (RAAN) |
| $\omega$ | argument of perigee |
| $A/m$ | effective area-to-mass ratio: projected area of the spacecraft perpendicular to the sun's ray divided by the mass of the spacecraft |
| $\Delta H$ | change in altitude |
| $\Delta V$ | delta velocity or total velocity change |

## 4.2 Abbreviated terms

| | |
|---|---|
| EGM | Earth gravitational model |
| EOMDP | end-of-mission disposal plan |
| GEO | geosynchronous (geostationary) Earth orbit |
| RAAN | right ascension of ascending node |

2) In some references, the $C_R$ is defined as the index of surface reflection.

## 5 Geosynchronous region

The geosynchronous region is a circular ring around the Earth in the equatorial plane. Within this region, an object in space moves along the ring at a mean angular rate that is equal or very close to the Earth's rotation, meaning that the satellite appears to be positioned over a fixed location on the ground.

Without so-called north-south station-keeping, the inclination of a GEO satellite will gradually cycle between 0° (equatorial orbit) and a maximum of approximately 14,6° and back again. In addition to maintaining the accuracy of its inclination, a GEO satellite must execute station-keeping manoeuvres to maintain longitudinal accuracy, so as to prevent a naturally occurring drift to the east or to the west caused by asymmetries in the Earth's gravitational field, unless the satellite is located at one of the two “gravity wells” on the geostationary arc.

Figure 1 shows a three-dimensional view of the geosynchronous ring with a cross-section defining the approximate size of the ring. Figure 2 gives the dimensions of three regions of the cross-section. The cross-section is defined by two axes: the latitudinal axis and radial axis. This plane of the cross-section is perpendicular to the Earth's equatorial plane.

The three concentric boxes shown in Figure 2 give the approximate boundaries for three types of orbits. The smallest box represents the region where a geostationary satellite will be confined under station-keeping, and the next larger box approximates the region where a geosynchronous satellite may be located when its inclination is not controlled but it remains under a mission-specified value. For example, the upper value for some specific geosynchronous missions may range from 3° to 5° depending on the ground user's antenna design. The largest box represents the inclination excursion region for a non-operational GEO satellite and the ±200 km protected region. For most communication satellites, the longitude station-keeping limit is ±0,1°.

## 6 Protected region

The GEO protected region, defined by ISO 24113 and indicated by Region B in Figure 1, includes the rectangular toroid centred on geostationary altitude, with an extent 200 km above and below this altitude and with inclination limits of +15° to −15°. While operations are usually conducted within about 75 km of geostationary altitude, the GEO protected region is extended in altitude to create a manoeuvre corridor for relocating spacecraft. Passivation of the disposed spacecraft is necessary to ensure that accidental explosions from on-board energy sources do not create debris that could re-enter the protected region.

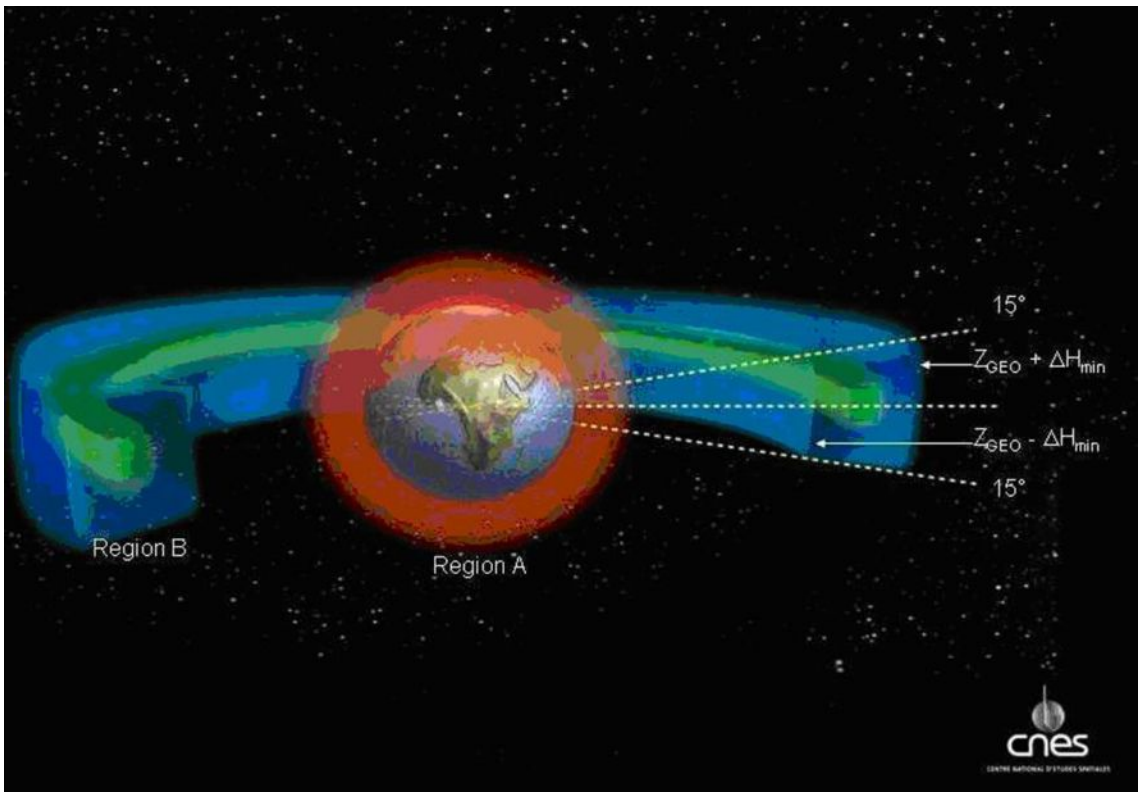


NOTE Reproduced by kind permission of the Centre National d'Études Spatiales.

**Figure 1 — Three-dimensional view of geosynchronous ring**

Dimensions in kilometres

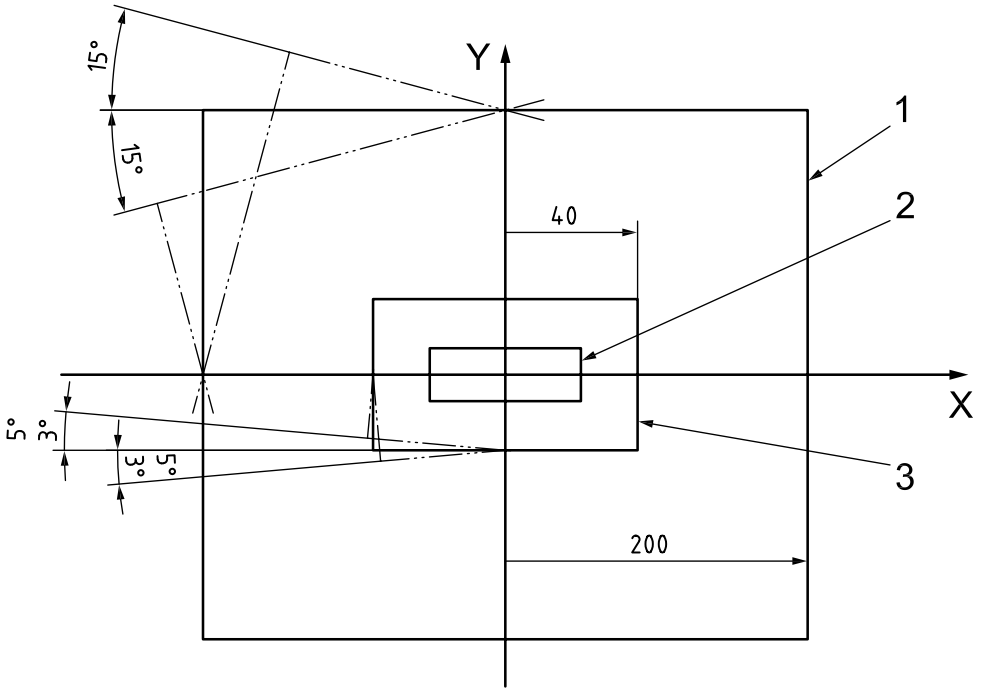


**Key**

X radial (away from Earth)

Y latitude (north)

1 protected region

2 geostationary control box (±37,5 km × ±37,5 km)

3 geosynchronous control box (±40 km radial; ±3° to ±5° in inclination)

NOTE The dimensions in the figure are not to scale.

**Figure 2 — Cross-section of the geosynchronous ring**

## 7 Primary requirements

### 7.1 Disposal manoeuvre planning

An EOMDP shall be developed, maintained and updated in all phases of mission and spacecraft design and operation. The EOMDP shall be an integral part of the space debris mitigation plan specified by ISO 24113. The EOMDP shall include the following:

a) details of the nominal mission orbit;

b) details of the targeted disposal orbit;

c) estimates of the propellant required for the disposal action;

d) identity of systems and capabilities required for successful completion of the disposal action;

e) criteria that, when met, shall dictate initiation of the disposal action;

f) identities of energy sources required to be depleted before end of life;

g) timeline for initiating and executing the disposal action;

h) timeline for depleting the remaining energy sources;

i) those individuals or entities, or individuals and entities to be notified of the end of mission and disposal and a timeline for notification.

### 7.2 Probability of successful disposal

In accordance with the requirements of ISO 24113:2010, 6.3.1, a spacecraft shall be designed such that the joint probability of having sufficient energy (propellant) remaining to achieve the final disposal orbit and successfully executing commands to deplete energy sources equals or exceeds 0,9 at the time disposal is executed. ISO 24113:2010, 6.3.1, also requires that the disposal success probability shall be evaluated as conditional probability (weighted on the mission success). Annex E provides a discussion of the conditional probability. Details of the design that provide the basis for the probability estimate shall be included in the EOMDP.

### 7.3 Criteria for executing disposal action

Specific criteria for initiating the disposal action shall be developed, included in the EOMDP and monitored throughout the mission life.

EXAMPLE Propellant amount remaining; redundancy remaining; status of electrical power; status of systems critical to a successful disposal action; time required to execute disposal action.

Projections of mission life based on these criteria shall be made as a regular part of mission status reviews.

### 7.4 Contingency planning

Independent of the success or failure of other aspects of a disposal action, a contingency plan shall be developed to deplete all energy sources and secure the vehicle before the final demise of the spacecraft. The objective shall be to ensure that actions necessary to secure the vehicle are taken before end of life. The contingency plan shall include criteria that define when the securing actions are to be taken, the rationale for each criterion, and a schedule for securing actions. The contingency plan shall be included in the EOMDP.

## 8 Disposal planning requirements

### 8.1 General

Planning activities for end-of-mission disposal shall start in the mission design phase. Planning for the actual disposal action should begin at least six months before the date of re-orbit manoeuvres. The steps described in 8.2 to 8.8 shall be followed in all mission phases and shall be documented in the EOMDP.

### 8.2 Estimating propellant reserves

The amount of fuel necessary to perform spacecraft disposal shall be estimated from the design phase, in accordance with the needed accuracy level, and reserved for the disposal phase. The minimum $\Delta V$ capability ($3-\sigma$) to reach the targeted disposal orbit shall be determined and specified in the EOMDP. The fuel required to provide this $\Delta V$ shall be maintained for end-of-life disposal[3)].

3) Further information will be provided in the future International Standard, ISO 23339.

## 8.3 Computing the initial perigee increase

In accordance with the requirements of ISO 24113:2010, 6.3.2, a spacecraft operating within the GEO protected region must, after completion of its GEO disposal manoeuvres, have an orbital state that satisfies at least one of the two conditions outlined below.

a) The orbit has an initial eccentricity of less than 0,003, and a minimum perigee altitude, $\Delta H$, expressed in kilometres, above the geostationary altitude (35 786 km) calculated according to Equation (1):

$$\Delta H = 235 + \left(1\,000 \times C_{\mathrm{R}} \times A/m\right) \tag{1}$$

The minimum value of $C_{\mathrm{R}}$ for computing the initial perigee increase shall be no less than 1,5 (a conservative estimate for $C_{\mathrm{R}}$, so as to adequately predict the solar radiation pressure effect). Justification shall be provided for using a value less than 1,5. Equation (1) was derived to ensure that the long-term perturbations will not cause the GEO debris to re-enter a protected zone of GEO plus 200 km.

b) The orbit has a perigee altitude sufficiently above the geostationary altitude that the spacecraft will not enter the GEO protected region within 100 years, irrespective of long-term perturbation forces.

## 8.4 Developing basic manoeuvre requirements for a stable disposal orbit

A stable disposal orbit shall be established by one of the two options described below.

a) Use Equation (1) and the eccentricity constraint to determine initial disposal orbit conditions.

b) Perform long-term (100-year) numerical integrations of the selected disposal orbit. The predicted minimum perigee altitude shall be greater than the 200 km protected region (see 8.5). It is recommended that the optimal eccentricity vector be determined from Tables A.1 to A.3, as a function of the date of orbital insertion and the value of $C_{\mathrm{R}} \times A/m$.

The altitude stability will be improved for either method if the following apply:

— the initial disposal perigee points toward the sun (perigee is sun-pointing);

— the disposal manoeuvres are performed in the most favourable season of the year, such that the same amount of perigee altitude increase will give the largest clearance over 100 years.

NOTE 1 The true optimal direction will differ slightly from the actual sun-pointing direction as a result of lunar perturbations.

NOTE 2 See Annex A for the optimal eccentricity and argument of perigee as a function of time for various values of $C_{\mathrm{R}} \times A/m$. Disposal orbits defined in accordance with Equation (1) are stable if the final eccentricity is less than 0,003. Tables A.1 to A.3 can be used to select the initial guess if option b) is used to determine the initial orbit parameters.

Should the intention be to operate the vehicle after placing it in a disposal orbit, the effects of such operation on the orbit shall be estimated, and this estimate and computations verifying that the operations will not compromise the long-term stability of the orbit (i.e. perigee shall remain above the protected region for 100 years) shall be included in the EOMDP. In all cases, the spacecraft shall be passivated (see 8.7) prior to end of life.

## 8.5 Developing long-term (100-year) disposal orbit characteristics

Long-term (100-year) orbit histories are needed only when the second option [see 8.4 b)] is chosen to establish a stable disposal orbit. If 8.4 b) is chosen, orbit propagation results developed by a reliable orbit propagator, either semi-analytic or numerical, shall be used to predict histories of perigee heights above GEO for a period of 100 years after initial insertion into the disposal orbit. The orbit propagator shall be of high precision and include as a minimum the perturbing forces of Earth's gravitational harmonics (up to a degree/order of 6 by 6), lunisolar attractions and solar radiation pressure. The precision of long-term

propagation of the propagator shall be verified against another well-established orbit propagator. Details on the orbit propagator used, assumptions made and analysis results shall be included in the EOMDP.

## 8.6 Determining the manoeuvre sequence

The manoeuvre sequence shall be determined that will place the GEO satellite in the required disposal orbit, have the optimal near-sun-pointing perigee and exhaust all the propellant on board. The disposal orbit is obtained after passivation and complete tank depletion, which can have unpredictable effects on orbital parameters and altitude. See Annex B for examples. The initial conditions of the disposal orbit shall be determined using the steps outlined in 8.4 and 8.5.

## 8.7 Developing a vehicle securing plan

Depletion of propellant creates forces that can affect a vehicle's orbit. The vehicle securing plan shall specify the following:

a) steps to deplete on-board energy sources after the satellite has been placed into the disposal orbit;

b) the effects the depletion action will have on the final orbit of the vehicle (the goal should be either to increase altitude or at least to limit a possible decrease in altitude);

c) criteria for when the plan will be executed; and

d) a schedule to be followed.

## 8.8 Developing a contingency plan

If a malfunction or other circumstance makes it necessary to proceed to the disposal phase earlier than planned, a contingency plan shall be developed that includes provisions for the following:

a) selecting an alternative orbit that is the least likely to interfere with the protected area (see Annex C): the contingency plan shall include criteria and techniques for selecting this orbit;

b) manoeuvring the satellite to the alternative orbit;

c) securing the satellite after the move; and

d) securing the vehicle if specified criteria are met at any time in the mission.

Annex D provides an example in which the quantity of propellant remaining is uncertain.

# Annex A
(informative)

# Tabulated values of the optimal eccentricity vector

Tables A.1 to A.3 contain the optimal eccentricity vector [eccentricity and argument of perigee plus RAAN (or longitude of periapsis)] as a function of time and a function of $(C_R \times A/m)$, expressed in square metres per kilogram, that will yield the highest perigee over the next 100 years. The optimal values were calculated in a brute-force fashion using increments of $2{,}3 \times 10^{-5}$ in eccentricity and 5° in longitude of periapsis. The benefit gained from using the optimal vector over the sun-pointing strategy varied from 0 km to 20 km (the average was approximately 9 km). However, if the sun-pointing strategy is chosen for the disposed vehicle, then the longitude of periapsis should be set equal to the value of the solar longitude (depicted as $L_S$ in Tables A.1 to A.3) with an eccentricity equal to $0{,}01 \times C_R \times A/m$. These charts can be interpolated to find the optimal vector for any particular satellite at a given time. However, the following should be noted when using these tables.

The initial conditions used to generate the data assumed a constant semi-major axis of 300 km above GEO (i.e. a constant $\Delta V$ was used in the disposal), mean anomaly of 180° (i.e. the last burn occurs at apogee, raising the perigee so that the eccentricity is equal to the tabulated value), an inclination of 7,74° (maximum at end of life if inclination drift is allowed) and an epoch of 0:00 Universal Time on the first day of each month. Additional analysis has shown that the optimal vector depends little upon these elements (the minimum perigee altitude may vary by approximately 2 km for each component), but if a high level of accuracy is required for a given disposal, the interpolated values found from the tables should be used as an initial guess so as to find the optimum for a particular disposal situation. The exception is the RAAN: in the search process, the initial RAAN was set to 62,3° and the argument of perigee was changed in 5° increments until the optimal value was found. Different RAANs were then checked and it was found that the relevant angular parameter was the argument of perigee plus RAAN; if this value is held constant, then the results will again be consistent with 1 km to 2 km, irrespective of the particular RAAN.

In addition, care should be taken if interpolating the values. In searching for optimal values in the angular argument, it was found that, at times, there was not one pure maximum, but multiple local maximums. As either the time or $C_R \times A/m$ advanced, the true maximum jumped from one peak to another. For example, consider the 2008-05-01 disposal. A $C_R \times A/m$ of 0,015 $m^2$/kg has an optimal eccentricity of 0,000 04 and a longitude of periapsis and 262,3°, whereas the $C_R \times A/m$ of 0,03 $m^2$/kg has optimal values of 0,000 09 and 37,3°. Linearly interpolating would imply optimal values of 0,000 057 and 307,3° for a $C_R \times A/m$ of 0,02 $m^2$/kg. Instead, the $C_R \times A/m = 0{,}02$ optimal value was actually 0,000 015 and 47,3°. In this case, the optimal point switched from one maximum to another, and therefore the intermediate maximum would actually be close to one point or the other.

Therefore, when confronted with angular changes greater than 90°, it is recommended that interpolation not be performed. Instead, the closer value should be used either directly or as a starting point for a more refined search.

A few final comments on the general behaviour of the system are warranted. When the $A/m$ was small ($C_R \times A/m < 0{,}01$), the optimal angle was pointed at the lunar apogee; when the $A/m$ was large ($C_R \times A/m > 0{,}03$), the solar radiation pressure force became dominant and the optimal angle was directed toward the sun.

**Table A.1 — Optimal eccentricity vector for $C_R \times A/m$ = 0,00 m²/kg, $C_R \times A/m$ = 0,005 m²/kg and $C_R \times A/m$ = 0,01 m²/kg**

| Year | Month | $L_S$ | $C_R \times A/m$ = 0,00 m²/kg | | $C_R \times A/m$ = 0,005 m²/kg | | $C_R \times A/m$ = 0,01 m²/kg | |
|---|---|---|---|---|---|---|---|---|
| | | (°) | $e$ | $\omega + \Omega$ | $e$ | $\omega + \Omega$ | $e$ | $\omega + \Omega$ |
| 2006 | 1 | 281 | 0,000 115 | 132,3 | 0,000 065 | 142,3 | 0,000 090 | 177,3 |
| | 2 | 314 | 0,000 140 | 112,3 | 0,000 115 | 102,3 | 0,000 065 | 102,3 |
| | 3 | 341 | 0,000 140 | 117,3 | 0,000 115 | 117,3 | 0,000 115 | 92,3 |
| | 4 | 10 | 0,000 140 | 142,3 | 0,000 115 | 132,3 | 0,000 090 | 117,3 |
| | 5 | 38 | 0,000 140 | 162,3 | 0,000 115 | 147,3 | 0,000 090 | 127,3 |
| | 6 | 68 | 0,000 115 | 177,3 | 0,000 115 | 167,3 | 0,000 090 | 122,3 |
| | 7 | 99 | 0,000 065 | 167,3 | 0,000 090 | 122,3 | 0,000 140 | 117,3 |
| | 8 | 131 | 0,000 090 | 142,3 | 0,000 140 | 137,3 | 0,000 190 | 137,3 |
| | 9 | 160 | 0,000 115 | 157,3 | 0,000 165 | 157,3 | 0,000 215 | 157,3 |
| | 10 | 187 | 0,000 090 | 167,3 | 0,000 140 | 172,3 | 0,000 215 | 177,3 |
| | 11 | 216 | 0,000 090 | 187,3 | 0,000 140 | 202,3 | 0,000 215 | 207,3 |
| | 12 | 246 | 0,000 165 | 177,3 | 0,000 115 | 207,3 | 0,000 165 | 222,3 |
| 2007 | 1 | 281 | 0,000 140 | 187,3 | 0,000 140 | 207,3 | 0,000 140 | 222,3 |
| | 2 | 314 | 0,000 165 | 207,3 | 0,000 165 | 217,3 | 0,000 165 | 232,3 |
| | 3 | 341 | 0,000 165 | 212,3 | 0,000 115 | 227,3 | 0,000 115 | 242,3 |
| | 4 | 10 | 0,000 090 | 217,3 | 0,000 065 | 237,3 | 0,000 040 | 257,3 |
| | 5 | 37 | 0,000 040 | 192,3 | 0,000 015 | 167,3 | 0,000 015 | 147,3 |
| | 6 | 68 | 0,000 115 | 192,3 | 0,000 090 | 172,3 | 0,000 115 | 162,3 |
| | 7 | 99 | 0,000 140 | 202,3 | 0,000 165 | 192,3 | 0,000 140 | 177,3 |
| | 8 | 130 | 0,000 190 | 222,3 | 0,000 165 | 212,3 | 0,000 140 | 197,3 |
| | 9 | 159 | 0,000 165 | 237,3 | 0,000 165 | 222,3 | 0,000 190 | 207,3 |
| | 10 | 186 | 0,000 115 | 207,3 | 0,000 165 | 212,3 | 0,000 240 | 212,3 |
| | 11 | 215 | 0,000 190 | 227,3 | 0,000 240 | 227,3 | 0,000 290 | 227,3 |
| | 12 | 246 | 0,000 165 | 232,3 | 0,000 215 | 237,3 | 0,000 290 | 242,3 |
| 2008 | 1 | 280 | 0,000 115 | 237,3 | 0,000 165 | 252,3 | 0,000 215 | 252,3 |
| | 2 | 313 | 0,000 090 | 222,3 | 0,000 115 | 247,3 | 0,000 140 | 262,3 |
| | 3 | 342 | 0,000 115 | 227,3 | 0,000 090 | 252,3 | 0,000 115 | 272,3 |
| | 4 | 10 | 0,000 140 | 227,3 | 0,000 115 | 242,3 | 0,000 065 | 267,3 |
| | 5 | 38 | 0,000 190 | 237,3 | 0,000 115 | 242,3 | 0,000 090 | 252,3 |
| | 6 | 69 | 0,000 165 | 247,3 | 0,000 115 | 247,3 | 0,000 040 | 242,3 |
| | 7 | 100 | 0,000 140 | 237,3 | 0,000 115 | 227,3 | 0,000 140 | 212,3 |
| | 8 | 131 | 0,000 215 | 237,3 | 0,000 240 | 232,3 | 0,000 215 | 222,3 |
| | 9 | 160 | 0,000 215 | 252,3 | 0,000 165 | 242,3 | 0,000 165 | 232,3 |
| | 10 | 187 | 0,000 140 | 262,3 | 0,000 165 | 247,3 | 0,000 190 | 237,3 |
| | 11 | 216 | 0,000 215 | 247,3 | 0,000 115 | 252,3 | 0,000 165 | 242,3 |
| | 12 | 247 | 0,000 090 | 237,3 | 0,000 140 | 242,3 | 0,000 190 | 247,3 |

**Table A.1** (*continued*)

| Year | Month | $L_S$ (°) | $C_R \times A/m = 0{,}00$ m²/kg | | $C_R \times A/m = 0{,}005$ m²/kg | | $C_R \times A/m = 0{,}01$ m²/kg | |
|---|---|---|---|---|---|---|---|---|
| | | | $e$ | $\omega + \Omega$ | $e$ | $\omega + \Omega$ | $e$ | $\omega + \Omega$ |
| 2009 | 1 | 280 | 0,000 140 | 242,3 | 0,000 165 | 252,3 | 0,000 265 | 257,3 |
| | 2 | 313 | 0,000 165 | 257,3 | 0,000 190 | 267,3 | 0,000 265 | 272,3 |
| | 3 | 342 | 0,000 165 | 262,3 | 0,000 190 | 272,3 | 0,000 215 | 287,3 |
| | 4 | 10 | 0,000 115 | 262,3 | 0,000 115 | 287,3 | 0,000 140 | 312,3 |
| | 5 | 38 | 0,000 115 | 252,3 | 0,000 065 | 267,3 | 0,000 040 | 347,3 |
| | 6 | 69 | 0,000 115 | 272,3 | 0,000 065 | 282,3 | 0,000 040 | 287,3 |
| | 7 | 100 | 0,000 090 | 287,3 | 0,000 040 | 277,3 | 0,000 015 | 272,3 |
| | 8 | 131 | 0,000 015 | 292,3 | 0,000 015 | 342,3 | 0,000 015 | 192,3 |
| | 9 | 160 | 0,000 040 | 267,3 | 0,000 040 | 227,3 | 0,000 090 | 222,3 |
| | 10 | 187 | 0,000 140 | 297,3 | 0,000 115 | 247,3 | 0,000 115 | 237,3 |
| | 11 | 216 | 0,000 115 | 282,3 | 0,000 140 | 272,3 | 0,000 165 | 262,3 |
| | 12 | 247 | 0,000 090 | 302,3 | 0,000 115 | 287,3 | 0,000 165 | 277,3 |
| 2010 | 1 | 280 | 0,000 040 | 33 2,3 | 0,000 040 | 277,3 | 0,000 115 | 282,3 |
| | 2 | 313 | 0,000 065 | 282,3 | 0,000 090 | 297,3 | 0,000 165 | 297,3 |
| | 3 | 341 | 0,000 040 | 302,3 | 0,000 090 | 312,3 | 0,000 140 | 307,3 |
| | 4 | 10 | 0,000 065 | 332,3 | 0,000 090 | 342,3 | 0,000 140 | 347,3 |
| | 5 | 38 | 0,000 090 | 352,3 | 0,000 115 | 7,3 | 0,000 165 | 7,3 |
| | 6 | 68 | 0,000 090 | 22,3 | 0,000 115 | 27,3 | 0,000 140 | 37,3 |
| | 7 | 99 | 0,000 065 | 27,3 | 0,000 090 | 47,3 | 0,000 115 | 57,3 |
| | 8 | 131 | 0,000 015 | 337,3 | 0,000 040 | 67,3 | 0,000 065 | 77,3 |
| | 9 | 160 | 0,000 065 | 342,3 | 0,000 015 | 352,3 | 0,000 015 | 322,3 |
| | 10 | 187 | 0,000 090 | 7,3 | 0,000 040 | 7,3 | 0,000 015 | 7,3 |
| | 11 | 216 | 0,000 140 | 37,3 | 0,000 090 | 32,3 | 0,000 040 | 32,3 |
| | 12 | 246 | 0,000 140 | 47,3 | 0,000 065 | 32,3 | 0,000 040 | 17,3 |
| 2011 | 1 | 279 | 0,000 140 | 27,3 | 0,000 140 | 12,3 | 0,000 140 | 357,3 |
| | 2 | 313 | 0,000 215 | 42,3 | 0,000 190 | 27,3 | 0,000 215 | 17,3 |
| | 3 | 341 | 0,000 215 | 47,3 | 0,000 215 | 32,3 | 0,000 265 | 27,3 |
| | 4 | 10 | 0,000 165 | 57,3 | 0,000 215 | 52,3 | 0,000 240 | 42,3 |
| | 5 | 37 | 0,000 115 | 57,3 | 0,000 165 | 57,3 | 0,000 215 | 52,3 |
| | 6 | 68 | 0,000 115 | 42,3 | 0,000 165 | 52,3 | 0,000 215 | 57,3 |
| | 7 | 99 | 0,000 190 | 37,3 | 0,000 190 | 47,3 | 0,000 215 | 57,3 |
| | 8 | 130 | 0,000 265 | 47,3 | 0,000 265 | 57,3 | 0,000 265 | 62,3 |
| | 9 | 159 | 0,000 265 | 62,3 | 0,000 265 | 72,3 | 0,000 290 | 77,3 |
| | 10 | 186 | 0,000 215 | 62,3 | 0,000 165 | 72,3 | 0,000 140 | 92,3 |
| | 11 | 215 | 0,000 265 | 57,3 | 0,000 190 | 57,3 | 0,000 165 | 62,3 |
| | 12 | 246 | 0,000 265 | 62,3 | 0,000 190 | 62,3 | 0,000 140 | 62,3 |

**Table A.1** (*continued*)

| Year | Month | $L_S$ (°) | $C_R \times A/m$ = 0,00 m²/kg | | $C_R \times A/m$ = 0,005 m²/kg | | $C_R \times A/m$ = 0,01 m²/kg | |
|---|---|---|---|---|---|---|---|---|
| | | | $e$ | $\omega + \Omega$ | $e$ | $\omega + \Omega$ | $e$ | $\omega + \Omega$ |
| 2012 | 1 | 279 | 0,000 240 | 72,3 | 0,000 190 | 67,3 | 0,000 140 | 57,3 |
| | 2 | 312 | 0,000 190 | 67,3 | 0,000 190 | 57,3 | 0,000 165 | 42,3 |
| | 3 | 342 | 0,000 190 | 67,3 | 0,000 215 | 52,3 | 0,000 215 | 42,3 |
| | 4 | 10 | 0,000 240 | 62,3 | 0,000 265 | 57,3 | 0,000 340 | 52,3 |
| | 5 | 38 | 0,000 315 | 67,3 | 0,000 340 | 62,3 | 0,000 415 | 62,3 |
| | 6 | 69 | 0,000 315 | 77,3 | 0,000 365 | 77,3 | 0,000 415 | 72,3 |
| | 7 | 100 | 0,000 240 | 72,3 | 0,000 290 | 77,3 | 0,000 390 | 82,3 |
| | 8 | 131 | 0,000 315 | 72,3 | 0,000 340 | 77,3 | 0,000 365 | 82,3 |
| | 9 | 160 | 0,000 340 | 82,3 | 0,000 340 | 87,3 | 0,000 340 | 92,3 |
| | 10 | 187 | 0,000 290 | 87,3 | 0,000 290 | 97,3 | 0,000 265 | 107,3 |
| | 11 | 216 | 0,000 215 | 87,3 | 0,000 215 | 102,3 | 0,000 190 | 112,3 |
| | 12 | 247 | 0,000 215 | 82,3 | 0,000 140 | 82,3 | 0,000 090 | 87,3 |
| 2013 | 1 | 279 | 0,000 290 | 77,3 | 0,000 240 | 72,3 | 0,000 190 | 62,3 |
| | 2 | 312 | 0,000 340 | 82,3 | 0,000 315 | 77,3 | 0,000 290 | 72,3 |
| | 3 | 342 | 0,000 340 | 87,3 | 0,000 340 | 82,3 | 0,000 315 | 77,3 |
| | 4 | 10 | 0,000 315 | 97,3 | 0,000 290 | 87,3 | 0,000 315 | 77,3 |
| | 5 | 38 | 0,000 290 | 92,3 | 0,000 315 | 87,3 | 0,000 365 | 82,3 |
| | 6 | 69 | 0,000 315 | 97,3 | 0,000 390 | 97,3 | 0,000 415 | 92,3 |
| | 7 | 100 | 0,000 290 | 107,3 | 0,000 340 | 102,3 | 0,000 390 | 102,3 |
| | 8 | 131 | 0,000 240 | 112,3 | 0,000 290 | 112,3 | 0,000 340 | 117,3 |
| | 9 | 160 | 0,000 215 | 107,3 | 0,000 240 | 117,3 | 0,000 290 | 122,3 |
| | 10 | 187 | 0,000 265 | 97,3 | 0,000 265 | 112,3 | 0,000 290 | 122,3 |
| | 11 | 216 | 0,000 340 | 102,3 | 0,000 315 | 112,3 | 0,000 265 | 122,3 |
| | 12 | 247 | 0,000 340 | 112,3 | 0,000 290 | 117,3 | 0,000 265 | 127,3 |
| 2014 | 1 | 280 | 0,000 265 | 117,3 | 0,000 215 | 127,3 | 0,000 165 | 132,3 |
| | 2 | 313 | 0,000 265 | 112,3 | 0,000 215 | 112,3 | 0,000 190 | 102,3 |
| | 3 | 341 | 0,000 290 | 117,3 | 0,000 265 | 107,3 | 0,000 240 | 102,3 |
| | 4 | 10 | 0,000 315 | 127,3 | 0,000 290 | 122,3 | 0,000 290 | 117,3 |
| | 5 | 38 | 0,000 315 | 137,3 | 0,000 290 | 132,3 | 0,000 265 | 122,3 |
| | 6 | 68 | 0,000 240 | 142,3 | 0,000 240 | 137,3 | 0,000 290 | 122,3 |
| | 7 | 99 | 0,000 190 | 137,3 | 0,000 265 | 127,3 | 0,000 265 | 127,3 |
| | 8 | 131 | 0,000 240 | 127,3 | 0,000 315 | 127,3 | 0,000 365 | 127,3 |
| | 9 | 160 | 0,000 265 | 137,3 | 0,000 315 | 137,3 | 0,000 365 | 142,3 |
| | 10 | 187 | 0,000 290 | 142,3 | 0,000 340 | 152,3 | 0,000 365 | 152,3 |
| | 11 | 216 | 0,000 265 | 152,3 | 0,000 290 | 157,3 | 0,000 315 | 167,3 |
| | 12 | 246 | 0,000 340 | 162,3 | 0,000 265 | 162,3 | 0,000 265 | 177,3 |

**Table A.1** (*continued*)

| Year | Month | $L_S$ (°) | $C_R \times A/m = 0{,}00$ m²/kg | | $C_R \times A/m = 0{,}005$ m²/kg | | $C_R \times A/m = 0{,}01$ m²/kg | |
|---|---|---|---|---|---|---|---|---|
| | | | $e$ | $\omega + \Omega$ | $e$ | $\omega + \Omega$ | $e$ | $\omega + \Omega$ |
| 2015 | 1 | 279 | 0,000 315 | 162,3 | 0,000 290 | 172,3 | 0,000 265 | 182,3 |
| | 2 | 313 | 0,000 265 | 177,3 | 0,000 240 | 182,3 | 0,000 215 | 192,3 |
| | 3 | 341 | 0,000 240 | 177,3 | 0,000 215 | 177,3 | 0,000 165 | 182,3 |
| | 4 | 10 | 0,000 190 | 172,3 | 0,000 165 | 162,3 | 0,000 090 | 162,3 |
| | 5 | 37 | 0,000 215 | 162,3 | 0,000 190 | 152,3 | 0,000 190 | 142,3 |
| | 6 | 68 | 0,000 290 | 162,3 | 0,000 315 | 152,3 | 0,000 340 | 142,3 |
| | 7 | 99 | 0,000 315 | 172,3 | 0,000 315 | 162,3 | 0,000 340 | 157,3 |
| | 8 | 130 | 0,000 315 | 182,3 | 0,000 340 | 177,3 | 0,000 365 | 172,3 |
| | 9 | 159 | 0,000 265 | 182,3 | 0,000 290 | 182,3 | 0,000 365 | 177,3 |
| | 10 | 186 | 0,000 290 | 187,3 | 0,000 340 | 187,3 | 0,000 415 | 187,3 |
| | 11 | 215 | 0,000 315 | 197,3 | 0,000 365 | 202,3 | 0,000 415 | 202,3 |
| | 12 | 246 | 0,000 290 | 202,3 | 0,000 340 | 212,3 | 0,000 365 | 212,3 |
| 2016 | 1 | 279 | 0,000 215 | 207,3 | 0,000 240 | 217,3 | 0,000 290 | 222,3 |
| | 2 | 312 | 0,000 240 | 192,3 | 0,000 215 | 207,3 | 0,000 215 | 217,3 |
| | 3 | 342 | 0,000 240 | 192,3 | 0,000 215 | 202,3 | 0,000 165 | 212,3 |
| | 4 | 10 | 0,000 290 | 202,3 | 0,000 240 | 202,3 | 0,000 190 | 202,3 |
| | 5 | 38 | 0,000 315 | 207,3 | 0,000 265 | 207,3 | 0,000 190 | 202,3 |
| | 6 | 69 | 0,000 290 | 217,3 | 0,000 240 | 207,3 | 0,000 190 | 207,3 |
| | 7 | 100 | 0,000 290 | 217,3 | 0,000 290 | 202,3 | 0,000 315 | 192,3 |
| | 8 | 131 | 0,000 340 | 222,3 | 0,000 365 | 212,3 | 0,000 365 | 207,3 |
| | 9 | 160 | 0,000 315 | 232,3 | 0,000 340 | 222,3 | 0,000 365 | 217,3 |
| | 10 | 187 | 0,000 265 | 237,3 | 0,000 290 | 232,3 | 0,000 315 | 227,3 |
| | 11 | 216 | 0,000 215 | 222,3 | 0,000 265 | 222,3 | 0,000 315 | 222,3 |
| | 12 | 247 | 0,000 240 | 222,3 | 0,000 290 | 222,3 | 0,000 340 | 232,3 |
| 2017 | 1 | 279 | 0,000 315 | 227,3 | 0,000 340 | 232,3 | 0,000 390 | 237,3 |
| | 2 | 312 | 0,000 340 | 237,3 | 0,000 365 | 242,3 | 0,000 390 | 252,3 |
| | 3 | 342 | 0,000 340 | 242,3 | 0,000 340 | 247,3 | 0,000 340 | 257,3 |
| | 4 | 10 | 0,000 290 | 242,3 | 0,000 265 | 252,3 | 0,000 240 | 257,3 |
| | 5 | 38 | 0,000 315 | 242,3 | 0,000 240 | 247,3 | 0,000 190 | 247,3 |
| | 6 | 69 | 0,000 315 | 252,3 | 0,000 265 | 252,3 | 0,000 215 | 252,3 |
| | 7 | 100 | 0,000 290 | 257,3 | 0,000 240 | 257,3 | 0,000 190 | 257,3 |
| | 8 | 131 | 0,000 215 | 257,3 | 0,000 190 | 247,3 | 0,000 190 | 232,3 |
| | 9 | 160 | 0,000 240 | 247,3 | 0,000 240 | 237,3 | 0,000 265 | 227,3 |
| | 10 | 187 | 0,000 265 | 247,3 | 0,000 315 | 242,3 | 0,000 340 | 237,3 |
| | 11 | 216 | 0,000 315 | 257,3 | 0,000 365 | 257,3 | 0,000 415 | 252,3 |
| | 12 | 247 | 0,000 290 | 267,3 | 0,000 365 | 262,3 | 0,000 390 | 262,3 |

**Table A.1** (*continued*)

| Year | Month | $L_S$ (°) | $C_R \times A/m$ = 0,00 m²/kg | | $C_R \times A/m$ = 0,005 m²/kg | | $C_R \times A/m$ = 0,01 m²/kg | |
|---|---|---|---|---|---|---|---|---|
| | | | $e$ | $\omega + \Omega$ | $e$ | $\omega + \Omega$ | $e$ | $\omega + \Omega$ |
| 2018 | 1 | 280 | 0,000 240 | 262,3 | 0,000 290 | 267,3 | 0,000 365 | 272,3 |
| | 2 | 313 | 0,000 315 | 262,3 | 0,000 340 | 272,3 | 0,000 365 | 277,3 |
| | 3 | 341 | 0,000 315 | 272,3 | 0,000 340 | 272,3 | 0,000 340 | 287,3 |
| | 4 | 10 | 0,000 290 | 282,3 | 0,000 290 | 292,3 | 0,000 315 | 297,3 |
| | 5 | 38 | 0,000 215 | 287,3 | 0,000 240 | 302,3 | 0,000 240 | 312,3 |
| | 6 | 68 | 0,000 165 | 287,3 | 0,000 115 | 302,3 | 0,000 090 | 312,3 |
| | 7 | 99 | 0,000 190 | 267,3 | 0,000 115 | 277,3 | 0,000 065 | 257,3 |
| | 8 | 131 | 0,000 240 | 277,3 | 0,000 215 | 267,3 | 0,000 165 | 267,3 |
| | 9 | 160 | 0,000 265 | 287,3 | 0,000 215 | 282,3 | 0,000 215 | 272,3 |
| | 10 | 187 | 0,000 240 | 297,3 | 0,000 215 | 277,3 | 0,000 215 | 272,3 |
| | 11 | 216 | 0,000 215 | 292,3 | 0,000 265 | 277,3 | 0,000 265 | 272,3 |
| | 12 | 246 | 0,000 240 | 302,3 | 0,000 290 | 292,3 | 0,000 315 | 282,3 |
| 2019 | 1 | 279 | 0,000 190 | 312,3 | 0,000 240 | 307,3 | 0,000 290 | 302,3 |
| | 2 | 313 | 0,000 140 | 327,3 | 0,000 190 | 322,3 | 0,000 240 | 322,3 |
| | 3 | 341 | 0,000 140 | 327,3 | 0,000 190 | 332,3 | 0,000 265 | 337,3 |
| | 4 | 10 | 0,000 115 | 312,3 | 0,000 140 | 332,3 | 0,000 190 | 337,3 |
| | 5 | 37 | 0,000 140 | 307,3 | 0,000 140 | 322,3 | 0,000 140 | 342,3 |
| | 6 | 68 | 0,000 190 | 312,3 | 0,000 165 | 327,3 | 0,000 190 | 342,3 |
| | 7 | 99 | 0,000 215 | 332,3 | 0,000 190 | 342,3 | 0,000 165 | 352,3 |
| | 8 | 130 | 0,000 165 | 347,3 | 0,000 115 | 352,3 | 0,000 140 | 12,3 |
| | 9 | 159 | 0,000 140 | 327,3 | 0,000 090 | 327,3 | 0,000 065 | 307,3 |
| | 10 | 186 | 0,000 165 | 342,3 | 0,000 115 | 332,3 | 0,000 090 | 322,3 |
| | 11 | 215 | 0,000 165 | 2,3 | 0,000 140 | 352,3 | 0,000 115 | 342,3 |
| | 12 | 246 | 0,000 165 | 12,3 | 0,000 140 | 357,3 | 0,000 115 | 342,3 |
| 2020 | 1 | 279 | 0,000 115 | 17,3 | 0,000 090 | 347,3 | 0,000 115 | 332,3 |
| | 2 | 312 | 0,000 090 | 352,3 | 0,000 140 | 342,3 | 0,000 190 | 337,3 |
| | 3 | 342 | 0,000 115 | 352,3 | 0,000 165 | 352,3 | 0,000 215 | 347,3 |
| | 4 | 10 | 0,000 165 | 7,3 | 0,000 215 | 7,3 | 0,000 265 | 7,3 |
| | 5 | 38 | 0,000 165 | 22,3 | 0,000 215 | 22,3 | 0,000 290 | 27,3 |
| | 6 | 69 | 0,000 165 | 32,3 | 0,000 190 | 42,3 | 0,000 265 | 47,3 |
| | 7 | 100 | 0,000 165 | 32,3 | 0,000 190 | 47,3 | 0,000 215 | 57,3 |
| | 8 | 131 | 0,000 240 | 37,3 | 0,000 240 | 52,3 | 0,000 240 | 57,3 |
| | 9 | 160 | 0,000 215 | 52,3 | 0,000 215 | 62,3 | 0,000 215 | 72,3 |
| | 10 | 187 | 0,000 165 | 62,3 | 0,000 140 | 72,3 | 0,000 140 | 87,3 |
| | 11 | 216 | 0,000 115 | 52,3 | 0,000 040 | 47,3 | 0,000 015 | 52,3 |
| | 12 | 247 | 0,000 115 | 37,3 | 0,000 090 | 27,3 | 0,000 090 | 12,3 |

**Table A.1** (*continued*)

| Year | Month | $L_S$ (°) | $C_R \times A/m = 0{,}00$ m²/kg | | $C_R \times A/m = 0{,}005$ m²/kg | | $C_R \times A/m = 0{,}01$ m²/kg | |
|---|---|---|---|---|---|---|---|---|
| | | | $e$ | $\omega + \Omega$ | $e$ | $\omega + \Omega$ | $e$ | $\omega + \Omega$ |
| 2021 | 1 | 279 | 0,000 215 | 47,3 | 0,000 215 | 37,3 | 0,000 190 | 22,3 |
| | 2 | 312 | 0,000 265 | 62,3 | 0,000 240 | 52,3 | 0,000 190 | 42,3 |
| | 3 | 342 | 0,000 265 | 67,3 | 0,000 265 | 57,3 | 0,000 265 | 52,3 |
| | 4 | 10 | 0,000 215 | 72,3 | 0,000 240 | 62,3 | 0,000 265 | 47,3 |
| | 5 | 38 | 0,000 215 | 67,3 | 0,000 290 | 62,3 | 0,000 365 | 57,3 |
| | 6 | 69 | 0,000 265 | 72,3 | 0,000 340 | 72,3 | 0,000 390 | 72,3 |
| | 7 | 100 | 0,000 265 | 77,3 | 0,000 290 | 82,3 | 0,000 365 | 82,3 |
| | 8 | 131 | 0,000 215 | 77,3 | 0,000 240 | 87,3 | 0,000 265 | 92,3 |
| | 9 | 160 | 0,000 190 | 72,3 | 0,000 190 | 87,3 | 0,000 215 | 97,3 |
| | 10 | 187 | 0,000 240 | 72,3 | 0,000 190 | 82,3 | 0,000 190 | 92,3 |
| | 11 | 216 | 0,000 290 | 77,3 | 0,000 240 | 82,3 | 0,000 215 | 87,3 |
| | 12 | 247 | 0,000 290 | 87,3 | 0,000 240 | 92,3 | 0,000 165 | 92,3 |
| 2022 | 1 | 280 | 0,000 240 | 87,3 | 0,000 190 | 82,3 | 0,000 140 | 72,3 |
| | 2 | 313 | 0,000 290 | 82,3 | 0,000 290 | 72,3 | 0,000 265 | 67,3 |
| | 3 | 341 | 0,000 290 | 87,3 | 0,000 290 | 77,3 | 0,000 315 | 67,3 |
| | 4 | 10 | 0,000 290 | 97,3 | 0,000 290 | 92,3 | 0,000 290 | 82,3 |
| | 5 | 38 | 0,000 240 | 102,3 | 0,000 265 | 92,3 | 0,000 290 | 87,3 |
| | 6 | 68 | 0,000 165 | 97,3 | 0,000 215 | 92,3 | 0,000 265 | 92,3 |
| | 7 | 99 | 0,000 190 | 87,3 | 0,000 215 | 92,3 | 0,000 290 | 92,3 |
| | 8 | 131 | 0,000 240 | 92,3 | 0,000 290 | 97,3 | 0,000 365 | 97,3 |
| | 9 | 160 | 0,000 315 | 97,3 | 0,000 340 | 102,3 | 0,000 340 | 112,3 |
| | 10 | 187 | 0,000 315 | 102,3 | 0,000 290 | 117,3 | 0,000 315 | 122,3 |
| | 11 | 216 | 0,000 240 | 102,3 | 0,000 215 | 107,3 | 0,000 190 | 122,3 |
| | 12 | 246 | 0,000 265 | 102,3 | 0,000 240 | 107,3 | 0,000 190 | 112,3 |
| 2023 | 1 | 279 | 0,000 215 | 117,3 | 0,000 165 | 117,3 | 0,000 115 | 127,3 |
| | 2 | 313 | 0,000 140 | 122,3 | 0,000 090 | 117,3 | 0,000 040 | 107,3 |
| | 3 | 341 | 0,000 140 | 122,3 | 0,000 090 | 117,3 | 0,000 090 | 82,3 |
| | 4 | 10 | 0,000 165 | 107,3 | 0,000 165 | 97,3 | 0,000 165 | 82,3 |
| | 5 | 37 | 0,000 190 | 112,3 | 0,000 240 | 102,3 | 0,000 265 | 87,3 |
| | 6 | 68 | 0,000 240 | 117,3 | 0,000 290 | 107,3 | 0,000 315 | 102,3 |
| | 7 | 99 | 0,000 190 | 127,3 | 0,000 240 | 122,3 | 0,000 290 | 117,3 |
| | 8 | 130 | 0,000 140 | 112,3 | 0,000 190 | 117,3 | 0,000 240 | 117,3 |
| | 9 | 159 | 0,000 190 | 117,3 | 0,000 190 | 127,3 | 0,000 265 | 127,3 |
| | 10 | 186 | 0,000 190 | 132,3 | 0,000 215 | 142,3 | 0,000 240 | 147,3 |
| | 11 | 215 | 0,000 165 | 152,3 | 0,000 190 | 167,3 | 0,000 215 | 172,3 |
| | 12 | 246 | 0,000 140 | 177,3 | 0,000 140 | 177,3 | 0,000 165 | 192,3 |

**Table A.1** (*continued*)

| Year | Month | $L_S$ (°) | $C_R \times A/m$ = 0,00 m²/kg | | $C_R \times A/m$ = 0,005 m²/kg | | $C_R \times A/m$ = 0,01 m²/kg | |
|---|---|---|---|---|---|---|---|---|
| | | | $e$ | $\omega + \Omega$ | $e$ | $\omega + \Omega$ | $e$ | $\omega + \Omega$ |
| 2024 | 1 | 279 | 0,000 090 | 132,3 | 0,000 065 | 177,3 | 0,000 090 | 207,3 |
| | 2 | 312 | 0,000 140 | 127,3 | 0,000 090 | 127,3 | 0,000 040 | 127,3 |
| | 3 | 342 | 0,000 140 | 137,3 | 0,000 090 | 132,3 | 0,000 065 | 117,3 |
| | 4 | 10 | 0,000 140 | 157,3 | 0,000 090 | 147,3 | 0,000 065 | 142,3 |
| | 5 | 38 | 0,000 115 | 172,3 | 0,000 090 | 152,3 | 0,000 090 | 117,3 |
| | 6 | 69 | 0,000 090 | 177,3 | 0,000 115 | 142,3 | 0,000 165 | 127,3 |
| | 7 | 100 | 0,000 115 | 177,3 | 0,000 140 | 162,3 | 0,000 165 | 152,3 |
| | 8 | 131 | 0,000 165 | 217,3 | 0,000 190 | 182,3 | 0,000 215 | 172,3 |
| | 9 | 160 | 0,000 140 | 207,3 | 0,000 165 | 197,3 | 0,000 215 | 192,3 |
| | 10 | 187 | 0,000 090 | 212,3 | 0,000 140 | 202,3 | 0,000 190 | 197,3 |
| | 11 | 216 | 0,000 090 | 172,3 | 0,000 115 | 197,3 | 0,000 165 | 202,3 |
| | 12 | 247 | 0,000 140 | 182,3 | 0,000 140 | 197,3 | 0,000 140 | 202,3 |
| 2025 | 1 | 279 | 0,000 165 | 197,3 | 0,000 165 | 217,3 | 0,000 190 | 222,3 |
| | 2 | 312 | 0,000 165 | 217,3 | 0,000 190 | 232,3 | 0,000 190 | 242,3 |
| | 3 | 342 | 0,000 190 | 227,3 | 0,000 190 | 242,3 | 0,000 165 | 252,3 |
| | 4 | 10 | 0,000 115 | 222,3 | 0,000 040 | 172,3 | 0,000 015 | 152,3 |
| | 5 | 38 | 0,000 165 | 217,3 | 0,000 090 | 212,3 | 0,000 040 | 187,3 |
| | 6 | 69 | 0,000 190 | 227,3 | 0,000 140 | 217,3 | 0,000 090 | 207,3 |
| | 7 | 100 | 0,000 165 | 232,3 | 0,000 140 | 222,3 | 0,000 115 | 212,3 |
| | 8 | 131 | 0,000 115 | 227,3 | 0,000 115 | 207,3 | 0,000 115 | 177,3 |
| | 9 | 160 | 0,000 115 | 222,3 | 0,000 140 | 207,3 | 0,000 190 | 192,3 |
| | 10 | 187 | 0,000 165 | 227,3 | 0,000 215 | 222,3 | 0,000 240 | 212,3 |
| | 11 | 216 | 0,000 190 | 237,3 | 0,000 240 | 232,3 | 0,000 315 | 232,3 |
| | 12 | 247 | 0,000 190 | 242,3 | 0,000 265 | 247,3 | 0,000 315 | 247,3 |

**Table A.2 — Optimal eccentricity vector for $C_R \times A/m$ = 0,015 m²/kg, $C_R \times A/m$ = 0,02 m²/kg and $C_R \times A/m$ = 0,03 m²/kg**

| Year | Month | $L_S$ | $C_R \times A/m$ = 0,015 m²/kg | | $C_R \times A/m$ = 0,02 m²/kg | | $C_R \times A/m$ = 0,03 m²/kg | |
|---|---|---|---|---|---|---|---|---|
| | | (°) | $e$ | $\omega + \Omega$ | $e$ | $\omega + \Omega$ | $e$ | $\omega + \Omega$ |
| 2006 | 1 | 281 | 0,000 065 | 187,3 | 0,000 090 | 207,3 | 0,000 115 | 237,3 |
| | 2 | 314 | 0,000 015 | 247,3 | 0,000 065 | 257,3 | 0,000 140 | 272,3 |
| | 3 | 341 | 0,000 090 | 77,3 | 0,000 065 | 67,3 | 0,000 040 | 357,3 |
| | 4 | 10 | 0,000 065 | 107,3 | 0,000 040 | 92,3 | 0,000 140 | 32,3 |
| | 5 | 38 | 0,000 090 | 127,3 | 0,000 140 | 82,3 | 0,000 215 | 67,3 |
| | 6 | 68 | 0,000 140 | 107,3 | 0,000 190 | 102,3 | 0,000 265 | 87,3 |
| | 7 | 99 | 0,000 190 | 117,3 | 0,000 240 | 117,3 | 0,000 365 | 107,3 |
| | 8 | 131 | 0,000 240 | 137,3 | 0,000 290 | 137,3 | 0,000 390 | 137,3 |
| | 9 | 160 | 0,000 265 | 157,3 | 0,000 315 | 162,3 | 0,000 415 | 162,3 |
| | 10 | 187 | 0,000 240 | 177,3 | 0,000 315 | 182,3 | 0,000 415 | 182,3 |
| | 11 | 216 | 0,000 240 | 207,3 | 0,000 290 | 207,3 | 0,000 415 | 212,3 |
| | 12 | 246 | 0,000 215 | 232,3 | 0,000 265 | 232,3 | 0,000 365 | 237,3 |
| 2007 | 1 | 281 | 0,000 190 | 232,3 | 0,000 215 | 242,3 | 0,000 290 | 257,3 |
| | 2 | 314 | 0,000 165 | 247,3 | 0,000 165 | 267,3 | 0,000 290 | 272,3 |
| | 3 | 341 | 0,000 115 | 257,3 | 0,000 140 | 272,3 | 0,000 140 | 312,3 |
| | 4 | 10 | 0,000 015 | 287,3 | 0,000 015 | 312,3 | 0,000 090 | 7,3 |
| | 5 | 37 | 0,000 040 | 112,3 | 0,000 040 | 87,3 | 0,000 115 | 67,3 |
| | 6 | 68 | 0,000 115 | 142,3 | 0,000 115 | 122,3 | 0,000 190 | 102,3 |
| | 7 | 99 | 0,000 165 | 172,3 | 0,000 165 | 157,3 | 0,000 215 | 132,3 |
| | 8 | 130 | 0,000 165 | 187,3 | 0,000 190 | 172,3 | 0,000 265 | 162,3 |
| | 9 | 159 | 0,000 190 | 197,3 | 0,000 265 | 192,3 | 0,000 365 | 177,3 |
| | 10 | 186 | 0,000 290 | 207,3 | 0,000 365 | 207,3 | 0,000 440 | 202,3 |
| | 11 | 215 | 0,000 340 | 227,3 | 0,000 365 | 222,3 | 0,000 465 | 222,3 |
| | 12 | 246 | 0,000 365 | 242,3 | 0,000 415 | 242,3 | 0,000 515 | 247,3 |
| 2008 | 1 | 280 | 0,000 265 | 257,3 | 0,000 315 | 262,3 | 0,000 440 | 267,3 |
| | 2 | 313 | 0,000 165 | 277,3 | 0,000 215 | 282,3 | 0,000 340 | 287,3 |
| | 3 | 342 | 0,000 115 | 287,3 | 0,000 165 | 302,3 | 0,000 265 | 312,3 |
| | 4 | 10 | 0,000 040 | 312,3 | 0,000 065 | 312,3 | 0,000 140 | 352,3 |
| | 5 | 38 | 0,000 040 | 262,3 | 0,000 015 | 47,3 | 0,000 090 | 37,3 |
| | 6 | 69 | 0,000 015 | 172,3 | 0,000 040 | 137,3 | 0,000 090 | 102,3 |
| | 7 | 100 | 0,000 140 | 187,3 | 0,000 140 | 172,3 | 0,000 190 | 152,3 |
| | 8 | 131 | 0,000 215 | 212,3 | 0,000 265 | 207,3 | 0,000 265 | 182,3 |
| | 9 | 160 | 0,000 190 | 222,3 | 0,000 215 | 207,3 | 0,000 290 | 197,3 |
| | 10 | 187 | 0,000 215 | 227,3 | 0,000 265 | 222,3 | 0,000 340 | 212,3 |
| | 11 | 216 | 0,000 240 | 237,3 | 0,000 290 | 232,3 | 0,000 415 | 232,3 |
| | 12 | 247 | 0,000 240 | 247,3 | 0,000 315 | 247,3 | 0,000 415 | 247,3 |

**Table A.2** (*continued*)

| Year | Month | $L_S$ | $C_R \times A/m$ = 0,015 m²/kg | | $C_R \times A/m$ = 0,02 m²/kg | | $C_R \times A/m$ = 0,03 m²/kg | |
|---|---|---|---|---|---|---|---|---|
| | | (°) | $e$ | $\omega + \Omega$ | $e$ | $\omega + \Omega$ | $e$ | $\omega + \Omega$ |
| 2009 | 1 | 280 | 0,000 315 | 262,3 | 0,000 315 | 262,3 | 0,000 440 | 267,3 |
| | 2 | 313 | 0,000 315 | 277,3 | 0,000 340 | 282,3 | 0,000 440 | 287,3 |
| | 3 | 342 | 0,000 265 | 292,3 | 0,000 290 | 297,3 | 0,000 365 | 307,3 |
| | 4 | 10 | 0,000 165 | 317,3 | 0,000 190 | 327,3 | 0,000 290 | 337,3 |
| | 5 | 38 | 0,000 090 | 357,3 | 0,000 115 | 7,3 | 0,000 215 | 12,3 |
| | 6 | 69 | 0,000 040 | 42,3 | 0,000 090 | 52,3 | 0,000 190 | 62,3 |
| | 7 | 100 | 0,000 015 | 102,3 | 0,000 065 | 102,3 | 0,000 190 | 97,3 |
| | 8 | 131 | 0,000 065 | 172,3 | 0,000 115 | 157,3 | 0,000 190 | 137,3 |
| | 9 | 160 | 0,000 115 | 207,3 | 0,000 115 | 187,3 | 0,000 240 | 187,3 |
| | 10 | 187 | 0,000 165 | 227,3 | 0,000 190 | 217,3 | 0,000 290 | 212,3 |
| | 11 | 216 | 0,000 215 | 252,3 | 0,000 265 | 247,3 | 0,000 340 | 242,3 |
| | 12 | 247 | 0,000 215 | 272,3 | 0,000 265 | 267,3 | 0,000 390 | 262,3 |
| 2010 | 1 | 280 | 0,000 165 | 282,3 | 0,000 240 | 282,3 | 0,000 340 | 282,3 |
| | 2 | 313 | 0,000 215 | 297,3 | 0,000 240 | 302,3 | 0,000 340 | 307,3 |
| | 3 | 341 | 0,000 165 | 332,3 | 0,000 215 | 332,3 | 0,000 340 | 332,3 |
| | 4 | 10 | 0,000 190 | 357,3 | 0,000 240 | 357,3 | 0,000 340 | 7,3 |
| | 5 | 38 | 0,000 190 | 17,3 | 0,000 240 | 27,3 | 0,000 340 | 32,3 |
| | 6 | 68 | 0,000 190 | 42,3 | 0,000 240 | 47,3 | 0,000 365 | 52,3 |
| | 7 | 99 | 0,000 190 | 67,3 | 0,000 240 | 72,3 | 0,000 290 | 82,3 |
| | 8 | 131 | 0,000 090 | 92,3 | 0,000 140 | 102,3 | 0,000 215 | 112,3 |
| | 9 | 160 | 0,000 040 | 142,3 | 0,000 090 | 152,3 | 0,000 190 | 147,3 |
| | 10 | 187 | 0,000 015 | 192,3 | 0,000 065 | 192,3 | 0,000 190 | 192,3 |
| | 11 | 216 | 0,000 015 | 262,3 | 0,000 065 | 257,3 | 0,000 165 | 242,3 |
| | 12 | 246 | 0,000 090 | 312,3 | 0,000 140 | 297,3 | 0,000 215 | 282,3 |
| 2011 | 1 | 279 | 0,000 165 | 347,3 | 0,000 215 | 337,3 | 0,000 265 | 322,3 |
| | 2 | 313 | 0,000 240 | 12,3 | 0,000 265 | 2,3 | 0,000 340 | 352,3 |
| | 3 | 341 | 0,000 290 | 22,3 | 0,000 315 | 17,3 | 0,000 390 | 7,3 |
| | 4 | 10 | 0,000 265 | 32,3 | 0,000 315 | 32,3 | 0,000 415 | 27,3 |
| | 5 | 37 | 0,000 265 | 47,3 | 0,000 315 | 47,3 | 0,000 440 | 47,3 |
| | 6 | 68 | 0,000 240 | 57,3 | 0,000 290 | 57,3 | 0,000 415 | 62,3 |
| | 7 | 99 | 0,000 290 | 62,3 | 0,000 290 | 67,3 | 0,000 415 | 77,3 |
| | 8 | 130 | 0,000 315 | 72,3 | 0,000 315 | 77,3 | 0,000 415 | 87,3 |
| | 9 | 159 | 0,000 290 | 87,3 | 0,000 340 | 97,3 | 0,000 340 | 107,3 |
| | 10 | 186 | 0,000 165 | 97,3 | 0,000 190 | 112,3 | 0,000 240 | 132,3 |
| | 11 | 215 | 0,000 065 | 62,3 | 0,000 040 | 177,3 | 0,000 090 | 177,3 |
| | 12 | 246 | 0,000 090 | 57,3 | 0,000 015 | 242,3 | 0,000 015 | 247,3 |

**Table A.2** (*continued*)

| Year | Month | $L_S$ | $C_R \times A/m$ = 0,015 m²/kg | | $C_R \times A/m$ = 0,02 m²/kg | | $C_R \times A/m$ = 0,03 m²/kg | |
|---|---|---|---|---|---|---|---|---|
| | | (°) | $e$ | $\omega + \Omega$ | $e$ | $\omega + \Omega$ | $e$ | $\omega + \Omega$ |
| 2012 | 1 | 279 | 0,000 090 | 42,3 | 0,000 090 | 12,3 | 0,000 140 | 317,3 |
| | 2 | 312 | 0,000 165 | 22,3 | 0,000 190 | 12,3 | 0,000 265 | 357,3 |
| | 3 | 342 | 0,000 240 | 32,3 | 0,000 290 | 22,3 | 0,000 390 | 17,3 |
| | 4 | 10 | 0,000 390 | 47,3 | 0,000 440 | 42,3 | 0,000 515 | 37,3 |
| | 5 | 38 | 0,000 440 | 57,3 | 0,000 515 | 57,3 | 0,000 615 | 57,3 |
| | 6 | 69 | 0,000 465 | 72,3 | 0,000 515 | 72,3 | 0,000 640 | 72,3 |
| | 7 | 100 | 0,000 415 | 82,3 | 0,000 515 | 87,3 | 0,000 590 | 87,3 |
| | 8 | 131 | 0,000 365 | 87,3 | 0,000 415 | 92,3 | 0,000 515 | 97,3 |
| | 9 | 160 | 0,000 365 | 102,3 | 0,000 390 | 102,3 | 0,000 465 | 117,3 |
| | 10 | 187 | 0,000 290 | 112,3 | 0,000 290 | 122,3 | 0,000 340 | 137,3 |
| | 11 | 216 | 0,000 165 | 127,3 | 0,000 190 | 137,3 | 0,000 215 | 162,3 |
| | 12 | 247 | 0,000 040 | 87,3 | 0,000 040 | 172,3 | 0,000 090 | 192,3 |
| 2013 | 1 | 279 | 0,000 165 | 57,3 | 0,000 115 | 32,3 | 0,000 015 | 247,3 |
| | 2 | 312 | 0,000 240 | 62,3 | 0,000 215 | 52,3 | 0,000 215 | 42,3 |
| | 3 | 342 | 0,000 340 | 67,3 | 0,000 340 | 62,3 | 0,000 365 | 47,3 |
| | 4 | 10 | 0,000 365 | 72,3 | 0,000 365 | 62,3 | 0,000 465 | 52,3 |
| | 5 | 38 | 0,000 440 | 77,3 | 0,000 465 | 72,3 | 0,000 565 | 67,3 |
| | 6 | 69 | 0,000 490 | 87,3 | 0,000 540 | 87,3 | 0,000 640 | 87,3 |
| | 7 | 100 | 0,000 465 | 102,3 | 0,000 515 | 102,3 | 0,000 615 | 102,3 |
| | 8 | 131 | 0,000 390 | 117,3 | 0,000 440 | 117,3 | 0,000 540 | 122,3 |
| | 9 | 160 | 0,000 315 | 127,3 | 0,000 365 | 132,3 | 0,000 465 | 137,3 |
| | 10 | 187 | 0,000 315 | 127,3 | 0,000 315 | 137,3 | 0,000 390 | 147,3 |
| | 11 | 216 | 0,000 290 | 127,3 | 0,000 290 | 137,3 | 0,000 290 | 162,3 |
| | 12 | 247 | 0,000 240 | 132,3 | 0,000 215 | 142,3 | 0,000 165 | 177,3 |
| 2014 | 1 | 280 | 0,000 140 | 142,3 | 0,000 115 | 162,3 | 0,000 090 | 187,3 |
| | 2 | 313 | 0,000 140 | 97,3 | 0,000 015 | 202,3 | 0,000 015 | 237,3 |
| | 3 | 341 | 0,000 215 | 92,3 | 0,000 215 | 82,3 | 0,000 215 | 62,3 |
| | 4 | 10 | 0,000 290 | 107,3 | 0,000 265 | 97,3 | 0,000 315 | 82,3 |
| | 5 | 38 | 0,000 290 | 112,3 | 0,000 315 | 102,3 | 0,000 365 | 92,3 |
| | 6 | 68 | 0,000 290 | 117,3 | 0,000 315 | 112,3 | 0,000 415 | 102,3 |
| | 7 | 99 | 0,000 365 | 117,3 | 0,000 390 | 117,3 | 0,000 515 | 117,3 |
| | 8 | 131 | 0,000 415 | 127,3 | 0,000 465 | 127,3 | 0,000 565 | 127,3 |
| | 9 | 160 | 0,000 415 | 142,3 | 0,000 490 | 142,3 | 0,000 590 | 147,3 |
| | 10 | 187 | 0,000 415 | 157,3 | 0,000 440 | 162,3 | 0,000 540 | 167,3 |
| | 11 | 216 | 0,000 365 | 172,3 | 0,000 390 | 177,3 | 0,000 515 | 187,3 |
| | 12 | 246 | 0,000 315 | 182,3 | 0,000 315 | 192,3 | 0,000 415 | 207,3 |

**Table A.2** (*continued*)

| Year | Month | $L_S$ | $C_R \times A/m$ = 0,015 m²/kg | | $C_R \times A/m$ = 0,02 m²/kg | | $C_R \times A/m$ = 0,03 m²/kg | |
|---|---|---|---|---|---|---|---|---|
| | | (°) | $e$ | $\omega + \Omega$ | $e$ | $\omega + \Omega$ | $e$ | $\omega + \Omega$ |
| 2015 | 1 | 279 | 0,000 240 | 192,3 | 0,000 265 | 197,3 | 0,000 265 | 217,3 |
| | 2 | 313 | 0,000190 | 202,3 | 0,000 165 | 212,3 | 0,000 165 | 227,3 |
| | 3 | 341 | 0,000 140 | 197,3 | 0,000 090 | 217,3 | 0,000 040 | 272,3 |
| | 4 | 10 | 0,000 090 | 132,3 | 0,000 065 | 107,3 | 0,000 115 | 72,3 |
| | 5 | 37 | 0,000 215 | 127,3 | 0,000 240 | 117,3 | 0,000 265 | 97,3 |
| | 6 | 68 | 0,000 340 | 137,3 | 0,000 315 | 127,3 | 0,000 390 | 117,3 |
| | 7 | 99 | 0,000 390 | 152,3 | 0,000 415 | 147,3 | 0,000 465 | 137,3 |
| | 8 | 130 | 0,000 390 | 167,3 | 0,000 415 | 162,3 | 0,000 465 | 157,3 |
| | 9 | 159 | 0,000 390 | 177,3 | 0,000 465 | 177,3 | 0,000 565 | 172,3 |
| | 10 | 186 | 0,000 465 | 187,3 | 0,000 515 | 187,3 | 0,000 615 | 187,3 |
| | 11 | 215 | 0,000 440 | 207,3 | 0,000 490 | 207,3 | 0,000 640 | 207,3 |
| | 12 | 246 | 0,000 415 | 217,3 | 0,000 465 | 222,3 | 0,000 565 | 227,3 |
| 2016 | 1 | 279 | 0,000 315 | 232,3 | 0,000 365 | 237,3 | 0,000 440 | 242,3 |
| | 2 | 312 | 0,000 215 | 232,3 | 0,000 215 | 242,3 | 0,000 290 | 262,3 |
| | 3 | 342 | 0,000 140 | 222,3 | 0,000 140 | 257,3 | 0,000 165 | 282,3 |
| | 4 | 10 | 0,000 140 | 202,3 | 0,000 090 | 207,3 | 0,000 015 | 332,3 |
| | 5 | 38 | 0,000 140 | 202,3 | 0,000 090 | 197,3 | 0,000 040 | 87,3 |
| | 6 | 69 | 0,000 190 | 182,3 | 0,000 165 | 167,3 | 0,000 240 | 142,3 |
| | 7 | 100 | 0,000 315 | 187,3 | 0,000 315 | 177,3 | 0,000 340 | 162,3 |
| | 8 | 131 | 0,000 365 | 202,3 | 0,000 390 | 192,3 | 0,000 440 | 182,3 |
| | 9 | 160 | 0,000 365 | 217,3 | 0,000 390 | 207,3 | 0,000 465 | 197,3 |
| | 10 | 187 | 0,000 365 | 217,3 | 0,000 390 | 217,3 | 0,000 490 | 212,3 |
| | 11 | 216 | 0,000 365 | 222,3 | 0,000 440 | 222,3 | 0,000 540 | 222,3 |
| | 12 | 247 | 0,000 390 | 232,3 | 0,000 440 | 232,3 | 0,000 540 | 237,3 |
| 2017 | 1 | 279 | 0,000 415 | 242,3 | 0,000 465 | 247,3 | 0,000 565 | 252,3 |
| | 2 | 312 | 0,000 415 | 257,3 | 0,000 440 | 262,3 | 0,000 540 | 267,3 |
| | 3 | 342 | 0,000 365 | 267,3 | 0,000 390 | 272,3 | 0,000 440 | 282,3 |
| | 4 | 10 | 0,000 240 | 277,3 | 0,000 240 | 282,3 | 0,000 265 | 302,3 |
| | 5 | 38 | 0,000 140 | 252,3 | 0,000 115 | 277,3 | 0,000 115 | 322,3 |
| | 6 | 69 | 0,000 165 | 252,3 | 0,000 015 | 252,3 | 0,000 015 | 37,3 |
| | 7 | 100 | 0,000 140 | 237,3 | 0,000 065 | 217,3 | 0,000 065 | 157,3 |
| | 8 | 131 | 0,000 190 | 207,3 | 0,000 190 | 202,3 | 0,000 215 | 182,3 |
| | 9 | 160 | 0,000 290 | 222,3 | 0,000 315 | 212,3 | 0,000 390 | 202,3 |
| | 10 | 187 | 0,000 365 | 232,3 | 0,000 415 | 227,3 | 0,000 515 | 222,3 |
| | 11 | 216 | 0,000 465 | 247,3 | 0,000 515 | 247,3 | 0,000 615 | 242,3 |
| | 12 | 247 | 0,000 440 | 262,3 | 0,000 490 | 262,3 | 0,000 640 | 257,3 |

**Table A.2** (*continued*)

| Year | Month | $L_S$ | $C_R \times A/m$ = 0,015 m²/kg | | $C_R \times A/m$ = 0,02 m²/kg | | $C_R \times A/m$ = 0,03 m²/kg | |
|---|---|---|---|---|---|---|---|---|
| | | (°) | $e$ | $\omega + \Omega$ | $e$ | $\omega + \Omega$ | $e$ | $\omega + \Omega$ |
| 2018 | 1 | 280 | 0,000 415 | 272,3 | 0,000 465 | 272,3 | 0,000 565 | 272,3 |
| | 2 | 313 | 0,000 415 | 277,3 | 0,000 440 | 282,3 | 0,000 565 | 287,3 |
| | 3 | 341 | 0,000 365 | 287,3 | 0,000 390 | 297,3 | 0,000 465 | 302,3 |
| | 4 | 10 | 0,000 315 | 307,3 | 0,000 340 | 312,3 | 0,000 390 | 327,3 |
| | 5 | 38 | 0,000 215 | 317,3 | 0,000 215 | 332,3 | 0,000 265 | 347,3 |
| | 6 | 68 | 0,000 090 | 332,3 | 0,000 115 | 352,3 | 0,000 140 | 22,3 |
| | 7 | 99 | 0,000 015 | 247,3 | 0,000 015 | 22,3 | 0,000 065 | 62,3 |
| | 8 | 131 | 0,000 140 | 262,3 | 0,000 115 | 232,3 | 0,000 015 | 122,3 |
| | 9 | 160 | 0,000 190 | 257,3 | 0,000 190 | 247,3 | 0,000 215 | 217,3 |
| | 10 | 187 | 0,000 215 | 262,3 | 0,000 265 | 247,3 | 0,000 340 | 227,3 |
| | 11 | 216 | 0,000 315 | 267,3 | 0,000 390 | 257,3 | 0,000 465 | 252,3 |
| | 12 | 246 | 0,000 365 | 282,3 | 0,000 415 | 277,3 | 0,000 515 | 272,3 |
| 2019 | 1 | 279 | 0,000 340 | 302,3 | 0,000 390 | 297,3 | 0,000 515 | 297,3 |
| | 2 | 313 | 0,000 290 | 317,3 | 0,000 340 | 317,3 | 0,000 465 | 317,3 |
| | 3 | 341 | 0,000 315 | 337,3 | 0,000 365 | 337,3 | 0,000 465 | 337,3 |
| | 4 | 10 | 0,000 215 | 347,3 | 0,000 265 | 352,3 | 0,000 390 | 357,3 |
| | 5 | 37 | 0,000 190 | 357,3 | 0,000 215 | 2,3 | 0,000 315 | 17,3 |
| | 6 | 68 | 0,000 165 | 352,3 | 0,000 165 | 7,3 | 0,000 215 | 32,3 |
| | 7 | 99 | 0,000 140 | 7,3 | 0,000 115 | 17,3 | 0,000 140 | 47,3 |
| | 8 | 130 | 0,000 140 | 27,3 | 0,000 115 | 37,3 | 0,000 115 | 67,3 |
| | 9 | 159 | 0,000 040 | 302,3 | 0,000 040 | 82,3 | 0,000 065 | 117,3 |
| | 10 | 186 | 0,000 065 | 307,3 | 0,000 015 | 147,3 | 0,000 040 | 162,3 |
| | 11 | 215 | 0,000 090 | 317,3 | 0,000 065 | 302,3 | 0,000 140 | 252,3 |
| | 12 | 246 | 0,000 090 | 317,3 | 0,000 115 | 302,3 | 0,000 215 | 277,3 |
| 2020 | 1 | 279 | 0,000 165 | 307,3 | 0,000 215 | 307,3 | 0,000 315 | 302,3 |
| | 2 | 312 | 0,000 265 | 337,3 | 0,000 315 | 327,3 | 0,000 415 | 322,3 |
| | 3 | 342 | 0,000 265 | 347,3 | 0,000 340 | 347,3 | 0,000 440 | 347,3 |
| | 4 | 10 | 0,000 315 | 12,3 | 0,000 365 | 12,3 | 0,000 490 | 12,3 |
| | 5 | 38 | 0,000 365 | 32,3 | 0,000 415 | 32,3 | 0,000 490 | 32,3 |
| | 6 | 69 | 0,000 315 | 52,3 | 0,000 365 | 57,3 | 0,000 490 | 57,3 |
| | 7 | 100 | 0,000 290 | 62,3 | 0,000 290 | 67,3 | 0,000 390 | 77,3 |
| | 8 | 131 | 0,000 215 | 72,3 | 0,000 240 | 77,3 | 0,000 340 | 92,3 |
| | 9 | 160 | 0,000 215 | 82,3 | 0,000 240 | 92,3 | 0,000 265 | 107,3 |
| | 10 | 187 | 0,000 115 | 107,3 | 0,000 115 | 112,3 | 0,000 140 | 137,3 |
| | 11 | 216 | 0,000 015 | 117,3 | 0,000 015 | 137,3 | 0,000 040 | 177,3 |
| | 12 | 247 | 0,000 090 | 357,3 | 0,000 090 | 337,3 | 0,000 115 | 302,3 |

**Table A.2** (*continued*)

| Year | Month | $L_S$ | $C_R \times A/m$ = 0,015 m²/kg | | $C_R \times A/m$ = 0,02 m²/kg | | $C_R \times A/m$ = 0,03 m²/kg | |
|---|---|---|---|---|---|---|---|---|
| | | (°) | $e$ | $\omega + \Omega$ | $e$ | $\omega + \Omega$ | $e$ | $\omega + \Omega$ |
| 2021 | 1 | 279 | 0,000 165 | 12,3 | 0,000 165 | 2,3 | 0,000 190 | 332,3 |
| | 2 | 312 | 0,000 215 | 27,3 | 0,000 240 | 17,3 | 0,000 290 | 357,3 |
| | 3 | 342 | 0,000 290 | 42,3 | 0,000 315 | 32,3 | 0,000 415 | 22,3 |
| | 4 | 10 | 0,000 315 | 47,3 | 0,000 390 | 42,3 | 0,000 465 | 37,3 |
| | 5 | 38 | 0,000 390 | 57,3 | 0,000 440 | 57,3 | 0,000 540 | 52,3 |
| | 6 | 69 | 0,000 440 | 72,3 | 0,000 490 | 72,3 | 0,000 615 | 72,3 |
| | 7 | 100 | 0,000 390 | 87,3 | 0,000 440 | 87,3 | 0,000 565 | 87,3 |
| | 8 | 131 | 0,000 315 | 102,3 | 0,000 365 | 102,3 | 0,000 465 | 107,3 |
| | 9 | 160 | 0,000 240 | 107,3 | 0,000 265 | 112,3 | 0,000 340 | 127,3 |
| | 10 | 187 | 0,000 165 | 112,3 | 0,000 190 | 122,3 | 0,000 240 | 142,3 |
| | 11 | 216 | 0,000 190 | 97,3 | 0,000 140 | 117,3 | 0,000 115 | 157,3 |
| | 12 | 247 | 0,000 140 | 102,3 | 0,000 115 | 102,3 | 0,000 015 | 272,3 |
| 2022 | 1 | 280 | 0,000 090 | 57,3 | 0,000 090 | 27,3 | 0,000 115 | 2,3 |
| | 2 | 313 | 0,000 240 | 57,3 | 0,000 240 | 47,3 | 0,000 240 | 32,3 |
| | 3 | 341 | 0,000 315 | 62,3 | 0,000 340 | 52,3 | 0,000 340 | 42,3 |
| | 4 | 10 | 0,000 315 | 72,3 | 0,000 340 | 67,3 | 0,000 415 | 57,3 |
| | 5 | 38 | 0,000 340 | 82,3 | 0,000 365 | 77,3 | 0,000 465 | 67,3 |
| | 6 | 68 | 0,000 315 | 87,3 | 0,000 365 | 87,3 | 0,000 490 | 82,3 |
| | 7 | 99 | 0,000 340 | 92,3 | 0,000 415 | 92,3 | 0,000 490 | 97,3 |
| | 8 | 131 | 0,000 390 | 102,3 | 0,000 465 | 102,3 | 0,000 515 | 112,3 |
| | 9 | 160 | 0,000 365 | 117,3 | 0,000 440 | 117,3 | 0,000 490 | 127,3 |
| | 10 | 187 | 0,000 315 | 132,3 | 0,000 365 | 137,3 | 0,000 440 | 147,3 |
| | 11 | 216 | 0,000 190 | 142,3 | 0,000 215 | 162,3 | 0,000 290 | 172,3 |
| | 12 | 246 | 0,000 140 | 132,3 | 0,000 090 | 157,3 | 0,000 140 | 197,3 |
| 2023 | 1 | 279 | 0,000 065 | 127,3 | 0,000 015 | 232,3 | 0,000 040 | 267,3 |
| | 2 | 313 | 0,000 040 | 67,3 | 0,000 040 | 32,3 | 0,000 115 | 352,3 |
| | 3 | 341 | 0,000 090 | 62,3 | 0,000 090 | 42,3 | 0,000 190 | 27,3 |
| | 4 | 10 | 0,000 190 | 77,3 | 0,000 240 | 67,3 | 0,000 290 | 52,3 |
| | 5 | 37 | 0,000 315 | 82,3 | 0,000 390 | 77,3 | 0,000 440 | 72,3 |
| | 6 | 68 | 0,000 365 | 102,3 | 0,000 415 | 97,3 | 0,000 515 | 92,3 |
| | 7 | 99 | 0,000 340 | 117,3 | 0,000 390 | 112,3 | 0,000 490 | 112,3 |
| | 8 | 130 | 0,000 290 | 117,3 | 0,000 365 | 117,3 | 0,000 465 | 122,3 |
| | 9 | 159 | 0,000 315 | 127,3 | 0,000 365 | 137,3 | 0,000 440 | 142,3 |
| | 10 | 186 | 0,000 265 | 152,3 | 0,000 315 | 162,3 | 0,000 415 | 167,3 |
| | 11 | 215 | 0,000 240 | 182,3 | 0,000 265 | 182,3 | 0,000 365 | 192,3 |
| | 12 | 246 | 0,000 215 | 207,3 | 0,000 240 | 212,3 | 0,000 340 | 222,3 |

**Table A.2** (*continued*)

| Year | Month | $L_S$ | $C_R \times A/m$ = 0,015 m²/kg | | $C_R \times A/m$ = 0,02 m²/kg | | $C_R \times A/m$ = 0,03 m²/kg | |
|---|---|---|---|---|---|---|---|---|
| | | (°) | $e$ | $\omega + \Omega$ | $e$ | $\omega + \Omega$ | $e$ | $\omega + \Omega$ |
| 2024 | 1 | 279 | 0,000 090 | 227,3 | 0,000 140 | 237,3 | 0,000 215 | 247,3 |
| | 2 | 312 | 0,000 015 | 97,3 | 0,000 040 | 287,3 | 0,000 140 | 297,3 |
| | 3 | 342 | 0,000 015 | 97,3 | 0,000 015 | 317,3 | 0,000 115 | 337,3 |
| | 4 | 10 | 0,000 040 | 117,3 | 0,000 090 | 52,3 | 0,000 165 | 37,3 |
| | 5 | 38 | 0,000 165 | 87,3 | 0,000 190 | 82,3 | 0,000 290 | 67,3 |
| | 6 | 69 | 0,000 190 | 122,3 | 0,000 265 | 112,3 | 0,000 315 | 102,3 |
| | 7 | 100 | 0,000 240 | 142,3 | 0,000 290 | 137,3 | 0,000 365 | 127,3 |
| | 8 | 131 | 0,000 240 | 162,3 | 0,000 290 | 162,3 | 0,000 365 | 152,3 |
| | 9 | 160 | 0,000 240 | 182,3 | 0,000 290 | 182,3 | 0,000 390 | 177,3 |
| | 10 | 187 | 0,000 240 | 197,3 | 0,000 290 | 197,3 | 0,000 390 | 192,3 |
| | 11 | 216 | 0,000 215 | 207,3 | 0,000 240 | 207,3 | 0,000 365 | 212,3 |
| | 12 | 247 | 0,000 215 | 222,3 | 0,000 240 | 222,3 | 0,000 340 | 232,3 |
| 2025 | 1 | 279 | 0,000 215 | 232,3 | 0,000 240 | 237,3 | 0,000 315 | 252,3 |
| | 2 | 312 | 0,000 215 | 252,3 | 0,000 240 | 257,3 | 0,000 290 | 272,3 |
| | 3 | 342 | 0,000 190 | 262,3 | 0,000 165 | 277,3 | 0,000 240 | 292,3 |
| | 4 | 10 | 0,000 015 | 142,3 | 0,000 065 | 317,3 | 0,000 165 | 327,3 |
| | 5 | 38 | 0,000 015 | 187,3 | 0,000 015 | 352,3 | 0,000 065 | 17,3 |
| | 6 | 69 | 0,000 065 | 212,3 | 0,000 065 | 102,3 | 0,000 115 | 87,3 |
| | 7 | 100 | 0,000 065 | 187,3 | 0,000 090 | 147,3 | 0,000 215 | 127,3 |
| | 8 | 131 | 0,000 165 | 177,3 | 0,000 215 | 167,3 | 0,000 290 | 152,3 |
| | 9 | 160 | 0,000 215 | 192,3 | 0,000 265 | 182,3 | 0,000 365 | 182,3 |
| | 10 | 187 | 0,000 265 | 207,3 | 0,000 340 | 207,3 | 0,000 440 | 202,3 |
| | 11 | 216 | 0,000 390 | 232,3 | 0,000 390 | 227,3 | 0,000 515 | 227,3 |
| | 12 | 247 | 0,000 365 | 247,3 | 0,000 440 | 247,3 | 0,000 540 | 247,3 |

**Table A.3 — Optimal eccentricity vector for $C_R \times A/m$ = 0,04 m²/kg, $C_R \times A/m$ = 0,05 m²/kg and $C_R \times A/m$ = 0,06 m²/kg**

| Year | Month | $L_S$ | $C_R \times A/m$ = 0,04 m²/kg | | $C_R \times A/m$ = 0,05 m²/kg | | $C_R \times A/m$ = 0,06 m²/kg | |
|---|---|---|---|---|---|---|---|---|
| | | (°) | $e$ | $\omega + \Omega$ | $e$ | $\omega + \Omega$ | $e$ | $\omega + \Omega$ |
| 2006 | 1 | 281 | 0,000 215 | 252,3 | 0,000 315 | 257,3 | 0,000 415 | 267,3 |
| | 2 | 314 | 0,000 190 | 297,3 | 0,000 315 | 297,3 | 0,000 415 | 302,3 |
| | 3 | 341 | 0,000 165 | 352,3 | 0,000 265 | 347,3 | 0,000 390 | 347,3 |
| | 4 | 10 | 0,000 215 | 22,3 | 0,000 315 | 17,3 | 0,000 440 | 17,3 |
| | 5 | 38 | 0,000 315 | 57,3 | 0,000 415 | 52,3 | 0,000 540 | 52,3 |
| | 6 | 68 | 0,000 390 | 87,3 | 0,000 490 | 82,3 | 0,000 615 | 82,3 |
| | 7 | 99 | 0,000 465 | 107,3 | 0,000 590 | 107,3 | 0,000 665 | 107,3 |
| | 8 | 131 | 0,000 515 | 132,3 | 0,000 615 | 132,3 | 0,000 715 | 132,3 |
| | 9 | 160 | 0,000 515 | 162,3 | 0,000 615 | 162,3 | 0,000 715 | 157,3 |
| | 10 | 187 | 0,000 490 | 187,3 | 0,000 615 | 187,3 | 0,000 715 | 187,3 |
| | 11 | 216 | 0,000 515 | 212,3 | 0,000 615 | 217,3 | 0,000 715 | 217,3 |
| | 12 | 246 | 0,000 515 | 242,3 | 0,000 590 | 242,3 | 0,000 715 | 242,3 |
| 2007 | 1 | 281 | 0,000 390 | 262,3 | 0,000 490 | 267,3 | 0,000 615 | 267,3 |
| | 2 | 314 | 0,000 365 | 282,3 | 0,000 415 | 292,3 | 0,000 515 | 297,3 |
| | 3 | 341 | 0,000 265 | 322,3 | 0,000 365 | 327,3 | 0,000 465 | 332,3 |
| | 4 | 10 | 0,000 190 | 7,3 | 0,000 315 | 12,3 | 0,000 415 | 12,3 |
| | 5 | 37 | 0,000 215 | 57,3 | 0,000 315 | 52,3 | 0,000 415 | 47,3 |
| | 6 | 68 | 0,000 290 | 92,3 | 0,000 390 | 87,3 | 0,000 515 | 82,3 |
| | 7 | 99 | 0,000 315 | 117,3 | 0,000 440 | 112,3 | 0,000 515 | 112,3 |
| | 8 | 130 | 0,000 390 | 142,3 | 0,000 490 | 142,3 | 0,000 565 | 142,3 |
| | 9 | 159 | 0,000 465 | 177,3 | 0,000 565 | 177,3 | 0,000 640 | 172,3 |
| | 10 | 186 | 0,000 540 | 197,3 | 0,000 665 | 197,3 | 0,000 790 | 197,3 |
| | 11 | 215 | 0,000 590 | 222,3 | 0,000 690 | 222,3 | 0,000 815 | 222,3 |
| | 12 | 246 | 0,000 615 | 247,3 | 0,000 740 | 247,3 | 0,000 865 | 247,3 |
| 2008 | 1 | 280 | 0,000 540 | 267,3 | 0,000 665 | 272,3 | 0,000 765 | 272,3 |
| | 2 | 313 | 0,000 440 | 292,3 | 0,000 540 | 297,3 | 0,000 640 | 297,3 |
| | 3 | 342 | 0,000 365 | 317,3 | 0,000 465 | 322,3 | 0,000 565 | 327,3 |
| | 4 | 10 | 0,000 240 | 357,3 | 0,000 365 | 2,3 | 0,000 490 | 7,3 |
| | 5 | 38 | 0,000 215 | 42,3 | 0,000 315 | 42,3 | 0,000 440 | 42,3 |
| | 6 | 69 | 0,000 140 | 92,3 | 0,000 315 | 82,3 | 0,000 390 | 82,3 |
| | 7 | 100 | 0,000 240 | 132,3 | 0,000 340 | 127,3 | 0,000 440 | 117,3 |
| | 8 | 131 | 0,000 315 | 167,3 | 0,000 390 | 162,3 | 0,000 465 | 152,3 |
| | 9 | 160 | 0,000 365 | 187,3 | 0,000 440 | 182,3 | 0,000 540 | 172,3 |
| | 10 | 187 | 0,000 440 | 207,3 | 0,000 540 | 202,3 | 0,000 665 | 202,3 |
| | 11 | 216 | 0,000 490 | 227,3 | 0,000 615 | 227,3 | 0,000 740 | 227,3 |
| | 12 | 247 | 0,000 540 | 247,3 | 0,000 690 | 252,3 | 0,000 790 | 252,3 |

**Table A.3** (*continued*)

| Year | Month | $L_S$ (°) | $C_R \times A/m = 0{,}04$ m²/kg | | $C_R \times A/m = 0{,}05$ m²/kg | | $C_R \times A/m = 0{,}06$ m²/kg | |
|---|---|---|---|---|---|---|---|---|
| | | | $e$ | $\omega + \Omega$ | $e$ | $\omega + \Omega$ | $e$ | $\omega + \Omega$ |
| 2009 | 1 | 280 | 0,000 565 | 272,3 | 0,000 665 | 272,3 | 0,000 790 | 272,3 |
| | 2 | 313 | 0,000 515 | 292,3 | 0,000 640 | 297,3 | 0,000 740 | 297,3 |
| | 3 | 342 | 0,000 465 | 312,3 | 0,000 540 | 322,3 | 0,000 640 | 322,3 |
| | 4 | 10 | 0,000 390 | 347,3 | 0,000 490 | 352,3 | 0,000 590 | 357,3 |
| | 5 | 38 | 0,000 290 | 22,3 | 0,000 415 | 27,3 | 0,000 540 | 32,3 |
| | 6 | 69 | 0,000 315 | 62,3 | 0,000 415 | 67,3 | 0,000 515 | 67,3 |
| | 7 | 100 | 0,000 290 | 97,3 | 0,000 390 | 97,3 | 0,000 515 | 97,3 |
| | 8 | 131 | 0,000 290 | 137,3 | 0,000 390 | 137,3 | 0,000 490 | 137,3 |
| | 9 | 160 | 0,000 315 | 177,3 | 0,000 415 | 172,3 | 0,000 515 | 172,3 |
| | 10 | 187 | 0,000 390 | 207,3 | 0,000 465 | 202,3 | 0,000 590 | 202,3 |
| | 11 | 216 | 0,000 415 | 237,3 | 0,000 490 | 232,3 | 0,000 615 | 232,3 |
| | 12 | 247 | 0,000 515 | 262,3 | 0,000 615 | 257,3 | 0,000 715 | 257,3 |
| 2010 | 1 | 280 | 0,000 465 | 282,3 | 0,000 565 | 282,3 | 0,000 690 | 282,3 |
| | 2 | 313 | 0,000 440 | 312,3 | 0,000 565 | 307,3 | 0,000 665 | 312,3 |
| | 3 | 341 | 0,000 440 | 337,3 | 0,000 540 | 337,3 | 0,000 615 | 342,3 |
| | 4 | 10 | 0,000 465 | 7,3 | 0,000 565 | 7,3 | 0,000 665 | 7,3 |
| | 5 | 38 | 0,000 440 | 32,3 | 0,000 565 | 32,3 | 0,000 665 | 37,3 |
| | 6 | 68 | 0,000 465 | 57,3 | 0,000 590 | 62,3 | 0,000 715 | 62,3 |
| | 7 | 99 | 0,000 440 | 82,3 | 0,000 515 | 87,3 | 0,000 590 | 87,3 |
| | 8 | 131 | 0,000 315 | 117,3 | 0,000 440 | 117,3 | 0,000 540 | 122,3 |
| | 9 | 160 | 0,000 290 | 152,3 | 0,000 390 | 152,3 | 0,000 490 | 152,3 |
| | 10 | 187 | 0,000 290 | 192,3 | 0,000 390 | 192,3 | 0,000 490 | 192,3 |
| | 11 | 216 | 0,000 290 | 237,3 | 0,000 390 | 232,3 | 0,000 490 | 232,3 |
| | 12 | 246 | 0,000 290 | 272,3 | 0,000 440 | 267,3 | 0,000 515 | 267,3 |
| 2011 | 1 | 279 | 0,000 340 | 312,3 | 0,000 490 | 302,3 | 0,000 515 | 302,3 |
| | 2 | 313 | 0,000 440 | 342,3 | 0,000 515 | 337,3 | 0,000 615 | 332,3 |
| | 3 | 341 | 0,000 490 | 2,3 | 0,000 615 | 2,3 | 0,000 690 | 357,3 |
| | 4 | 10 | 0,000 515 | 22,3 | 0,000 615 | 22,3 | 0,000 740 | 22,3 |
| | 5 | 37 | 0,000 540 | 47,3 | 0,000 665 | 47,3 | 0,000 790 | 47,3 |
| | 6 | 68 | 0,000 565 | 67,3 | 0,000 665 | 67,3 | 0,000 765 | 67,3 |
| | 7 | 99 | 0,000 490 | 82,3 | 0,000 565 | 87,3 | 0,000 665 | 87,3 |
| | 8 | 130 | 0,000 465 | 97,3 | 0,000 540 | 102,3 | 0,000 640 | 107,3 |
| | 9 | 159 | 0,000 415 | 117,3 | 0,000 490 | 122,3 | 0,000 590 | 127,3 |
| | 10 | 186 | 0,000 290 | 142,3 | 0,000 365 | 152,3 | 0,000 465 | 162,3 |
| | 11 | 215 | 0,000 165 | 197,3 | 0,000 265 | 202,3 | 0,000 365 | 207,3 |
| | 12 | 246 | 0,000 140 | 247,3 | 0,000 265 | 247,3 | 0,000 390 | 247,3 |

**Table A.3** (*continued*)

| Year | Month | $L_S$ (°) | $C_R \times A/m$ = 0,04 m²/kg | | $C_R \times A/m$ = 0,05 m²/kg | | $C_R \times A/m$ = 0,06 m²/kg | |
|---|---|---|---|---|---|---|---|---|
| | | | $e$ | $\omega + \Omega$ | $e$ | $\omega + \Omega$ | $e$ | $\omega + \Omega$ |
| 2012 | 1 | 279 | 0,000 240 | 307,3 | 0,000 340 | 297,3 | 0,000 440 | 297,3 |
| | 2 | 312 | 0,000 365 | 347,3 | 0,000 465 | 337,3 | 0,000 540 | 337,3 |
| | 3 | 342 | 0,000 440 | 7,3 | 0,000 565 | 7,3 | 0,000 665 | 2,3 |
| | 4 | 10 | 0,000 615 | 32,3 | 0,000 715 | 32,3 | 0,000 815 | 27,3 |
| | 5 | 38 | 0,000 715 | 52,3 | 0,000 840 | 52,3 | 0,000 965 | 52,3 |
| | 6 | 69 | 0,000 740 | 72,3 | 0,000 865 | 72,3 | 0,000 965 | 72,3 |
| | 7 | 100 | 0,000 665 | 87,3 | 0,000 815 | 92,3 | 0,000 915 | 92,3 |
| | 8 | 131 | 0,000 615 | 102,3 | 0,000 715 | 107,3 | 0,000 790 | 107,3 |
| | 9 | 160 | 0,000 540 | 122,3 | 0,000 590 | 132,3 | 0,000 690 | 132,3 |
| | 10 | 187 | 0,000 415 | 142,3 | 0,000 490 | 152,3 | 0,000 565 | 157,3 |
| | 11 | 216 | 0,000 265 | 177,3 | 0,000 340 | 187,3 | 0,000 440 | 197,3 |
| | 12 | 247 | 0,000 140 | 217,3 | 0,000 215 | 222,3 | 0,000 315 | 232,3 |
| 2013 | 1 | 279 | 0,000 090 | 302,3 | 0,000 165 | 302,3 | 0,000 340 | 292,3 |
| | 2 | 312 | 0,000 240 | 12,3 | 0,000 315 | 347,3 | 0,000 415 | 342,3 |
| | 3 | 342 | 0,000 390 | 27,3 | 0,000 465 | 17,3 | 0,000 565 | 7,3 |
| | 4 | 10 | 0,000 565 | 47,3 | 0,000 640 | 37,3 | 0,000 740 | 37,3 |
| | 5 | 38 | 0,000 665 | 62,3 | 0,000 815 | 62,3 | 0,000 865 | 57,3 |
| | 6 | 69 | 0,000 740 | 82,3 | 0,000 840 | 82,3 | 0,000 940 | 82,3 |
| | 7 | 100 | 0,000 715 | 102,3 | 0,000 815 | 102,3 | 0,000 915 | 102,3 |
| | 8 | 131 | 0,000 640 | 122,3 | 0,000 765 | 122,3 | 0,000 865 | 122,3 |
| | 9 | 160 | 0,000 565 | 142,3 | 0,000 665 | 142,3 | 0,000 740 | 147,3 |
| | 10 | 187 | 0,000 465 | 157,3 | 0,000 565 | 162,3 | 0,000 665 | 167,3 |
| | 11 | 216 | 0,000 340 | 177,3 | 0,000 415 | 187,3 | 0,000 515 | 192,3 |
| | 12 | 247 | 0,000 215 | 192,3 | 0,000 265 | 212,3 | 0,000 340 | 222,3 |
| 2014 | 1 | 280 | 0,000 090 | 222,3 | 0,000 140 | 242,3 | 0,000 240 | 257,3 |
| | 2 | 313 | 0,000 015 | 287,3 | 0,000 115 | 317,3 | 0,000 215 | 317,3 |
| | 3 | 341 | 0,000 240 | 42,3 | 0,000 290 | 27,3 | 0,000 365 | 22,3 |
| | 4 | 10 | 0,000 340 | 67,3 | 0,000 365 | 52,3 | 0,000 465 | 47,3 |
| | 5 | 38 | 0,000 440 | 82,3 | 0,000 515 | 72,3 | 0,000 615 | 67,3 |
| | 6 | 68 | 0,000 515 | 97,3 | 0,000 665 | 92,3 | 0,000 740 | 87,3 |
| | 7 | 99 | 0,000 615 | 112,3 | 0,000 765 | 107,3 | 0,000 865 | 107,3 |
| | 8 | 131 | 0,000 665 | 127,3 | 0,000 790 | 127,3 | 0,000 890 | 127,3 |
| | 9 | 160 | 0,000 690 | 147,3 | 0,000 740 | 152,3 | 0,000 865 | 152,3 |
| | 10 | 187 | 0,000 640 | 172,3 | 0,000 765 | 172,3 | 0,000 890 | 172,3 |
| | 11 | 216 | 0,000 590 | 192,3 | 0,000 690 | 197,3 | 0,000 815 | 202,3 |
| | 12 | 246 | 0,000 490 | 217,3 | 0,000 590 | 222,3 | 0,000 690 | 227,3 |

**Table A.3** (*continued*)

| Year | Month | $L_S$ (°) | $C_R \times A/m = 0{,}04$ m²/kg | | $C_R \times A/m = 0{,}05$ m²/kg | | $C_R \times A/m = 0{,}06$ m²/kg | |
|---|---|---|---|---|---|---|---|---|
| | | | $e$ | $\omega + \Omega$ | $e$ | $\omega + \Omega$ | $e$ | $\omega + \Omega$ |
| 2015 | 1 | 279 | 0,000 315 | 237,3 | 0,000 390 | 247,3 | 0,000 515 | 257,3 |
| | 2 | 313 | 0,000 190 | 272,3 | 0,000 240 | 277,3 | 0,000 340 | 287,3 |
| | 3 | 341 | 0,000 065 | 327,3 | 0,000 190 | 332,3 | 0,000 290 | 337,3 |
| | 4 | 10 | 0,000 190 | 52,3 | 0,000 265 | 37,3 | 0,000 365 | 32,3 |
| | 5 | 37 | 0,000 340 | 82,3 | 0,000 415 | 72,3 | 0,000 515 | 67,3 |
| | 6 | 68 | 0,000 490 | 112,3 | 0,000 540 | 102,3 | 0,000 640 | 97,3 |
| | 7 | 99 | 0,000 540 | 132,3 | 0,000 640 | 127,3 | 0,000 740 | 122,3 |
| | 8 | 130 | 0,000 590 | 152,3 | 0,000 715 | 147,3 | 0,000 790 | 147,3 |
| | 9 | 159 | 0,000 640 | 172,3 | 0,000 765 | 167,3 | 0,000 865 | 167,3 |
| | 10 | 186 | 0,000 740 | 187,3 | 0,000 840 | 187,3 | 0,000 940 | 187,3 |
| | 11 | 215 | 0,000 715 | 212,3 | 0,000 840 | 212,3 | 0,000 965 | 212,3 |
| | 12 | 246 | 0,000 690 | 227,3 | 0,000 765 | 232,3 | 0,000 890 | 232,3 |
| 2016 | 1 | 279 | 0,000 540 | 252,3 | 0,000 665 | 257,3 | 0,000 740 | 257,3 |
| | 2 | 312 | 0,000 390 | 272,3 | 0,000 465 | 282,3 | 0,000 565 | 287,3 |
| | 3 | 342 | 0,000 215 | 302,3 | 0,000 315 | 312,3 | 0,000 440 | 317,3 |
| | 4 | 10 | 0,000 090 | 7,3 | 0,000 190 | 12,3 | 0,000 315 | 12,3 |
| | 5 | 38 | 0,000 115 | 72,3 | 0,000 240 | 62,3 | 0,000 340 | 62,3 |
| | 6 | 69 | 0,000 265 | 127,3 | 0,000 340 | 112,3 | 0,000 415 | 102,3 |
| | 7 | 100 | 0,000 415 | 152,3 | 0,000 490 | 142,3 | 0,000 540 | 137,3 |
| | 8 | 131 | 0,000 515 | 177,3 | 0,000 565 | 167,3 | 0,000 665 | 162,3 |
| | 9 | 160 | 0,000 540 | 192,3 | 0,000 640 | 187,3 | 0,000 740 | 182,3 |
| | 10 | 187 | 0,000 615 | 207,3 | 0,000 690 | 207,3 | 0,000 790 | 207,3 |
| | 11 | 216 | 0,000 640 | 222,3 | 0,000 765 | 222,3 | 0,000 865 | 222,3 |
| | 12 | 247 | 0,000 665 | 242,3 | 0,000 765 | 242,3 | 0,000 890 | 242,3 |
| 2017 | 1 | 279 | 0,000 665 | 257,3 | 0,000 740 | 257,3 | 0,000 865 | 262,3 |
| | 2 | 312 | 0,000 615 | 277,3 | 0,000 690 | 282,3 | 0,000 765 | 287,3 |
| | 3 | 342 | 0,000 490 | 292,3 | 0,000 540 | 297,3 | 0,000 615 | 307,3 |
| | 4 | 10 | 0,000 340 | 317,3 | 0,000 390 | 327,3 | 0,000 490 | 337,3 |
| | 5 | 38 | 0,000 190 | 352,3 | 0,000 240 | 7,3 | 0,000 340 | 17,3 |
| | 6 | 69 | 0,000 090 | 62,3 | 0,000 215 | 67,3 | 0,000 340 | 67,3 |
| | 7 | 100 | 0,000 165 | 127,3 | 0,000 265 | 122,3 | 0,000 415 | 117,3 |
| | 8 | 131 | 0,000 315 | 167,3 | 0,000 390 | 162,3 | 0,000 465 | 152,3 |
| | 9 | 160 | 0,000 440 | 192,3 | 0,000 540 | 187,3 | 0,000 665 | 187,3 |
| | 10 | 187 | 0,000 615 | 217,3 | 0,000 715 | 212,3 | 0,000 815 | 207,3 |
| | 11 | 216 | 0,000 715 | 237,3 | 0,000 815 | 237,3 | 0,000 915 | 237,3 |
| | 12 | 247 | 0,000 740 | 257,3 | 0,000 840 | 257,3 | 0,000 940 | 257,3 |

**Table A.3** (*continued*)

| Year | Month | $L_S$ (°) | $C_R \times A/m$ = 0,04 m²/kg | | $C_R \times A/m$ = 0,05 m²/kg | | $C_R \times A/m$ = 0,06 m²/kg | |
|---|---|---|---|---|---|---|---|---|
| | | | $e$ | $\omega + \Omega$ | $e$ | $\omega + \Omega$ | $e$ | $\omega + \Omega$ |
| 2018 | 1 | 280 | 0,000 690 | 277,3 | 0,000 815 | 277,3 | 0,000 915 | 277,3 |
| | 2 | 313 | 0,000 640 | 292,3 | 0,000 740 | 292,3 | 0,000 840 | 297,3 |
| | 3 | 341 | 0,000 565 | 312,3 | 0,000 640 | 317,3 | 0,000 740 | 317,3 |
| | 4 | 10 | 0,000 440 | 337,3 | 0,000 515 | 342,3 | 0,000 615 | 347,3 |
| | 5 | 38 | 0,000 340 | 2,3 | 0,000 415 | 12,3 | 0,000 540 | 17,3 |
| | 6 | 68 | 0,000 215 | 37,3 | 0,000 315 | 47,3 | 0,000 440 | 52,3 |
| | 7 | 99 | 0,000 140 | 82,3 | 0,000 240 | 82,3 | 0,000 390 | 107,3 |
| | 8 | 131 | 0,000 140 | 152,3 | 0,000 240 | 147,3 | 0,000 340 | 142,3 |
| | 9 | 160 | 0,000 290 | 197,3 | 0,000 365 | 187,3 | 0,000 440 | 182,3 |
| | 10 | 187 | 0,000 415 | 222,3 | 0,000 515 | 217,3 | 0,000 615 | 212,3 |
| | 11 | 216 | 0,000 565 | 247,3 | 0,000 640 | 242,3 | 0,000 740 | 242,3 |
| | 12 | 246 | 0,000 615 | 272,3 | 0,000 740 | 267,3 | 0,000 840 | 267,3 |
| 2019 | 1 | 279 | 0,000 615 | 292,3 | 0,000 715 | 292,3 | 0,000 840 | 292,3 |
| | 2 | 313 | 0,000 565 | 317,3 | 0,000 690 | 317,3 | 0,000 815 | 317,3 |
| | 3 | 341 | 0,000 565 | 337,3 | 0,000 665 | 337,3 | 0,000 765 | 337,3 |
| | 4 | 10 | 0,000 490 | 2,3 | 0,000 590 | 2,3 | 0,000 690 | 2,3 |
| | 5 | 37 | 0,000 440 | 22,3 | 0,000 540 | 27,3 | 0,000 640 | 32,3 |
| | 6 | 68 | 0,000 315 | 42,3 | 0,000 415 | 52,3 | 0,000 515 | 57,3 |
| | 7 | 99 | 0,000 240 | 62,3 | 0,000 340 | 77,3 | 0,000 440 | 82,3 |
| | 8 | 130 | 0,000 165 | 97,3 | 0,000 240 | 102,3 | 0,000 340 | 117,3 |
| | 9 | 159 | 0,000 115 | 137,3 | 0,000 190 | 142,3 | 0,000 315 | 152,3 |
| | 10 | 186 | 0,000 115 | 182,3 | 0,000 240 | 192,3 | 0,000 365 | 192,3 |
| | 11 | 215 | 0,000 265 | 237,3 | 0,000 340 | 232,3 | 0,000 540 | 237,3 |
| | 12 | 246 | 0,000 315 | 272,3 | 0,000 440 | 262,3 | 0,000 615 | 267,3 |
| 2020 | 1 | 279 | 0,000 415 | 297,3 | 0,000 540 | 292,3 | 0,000 640 | 292,3 |
| | 2 | 312 | 0,000 515 | 322,3 | 0,000 615 | 322,3 | 0,000 715 | 317,3 |
| | 3 | 342 | 0,000 565 | 347,3 | 0,000 665 | 347,3 | 0,000 790 | 347,3 |
| | 4 | 10 | 0,000 590 | 12,3 | 0,000 690 | 12,3 | 0,000 815 | 12,3 |
| | 5 | 38 | 0,000 640 | 37,3 | 0,000 740 | 37,3 | 0,000 840 | 37,3 |
| | 6 | 69 | 0,000 590 | 62,3 | 0,000 715 | 62,3 | 0,000 865 | 62,3 |
| | 7 | 100 | 0,000 515 | 82,3 | 0,000 665 | 82,3 | 0,000 715 | 87,3 |
| | 8 | 131 | 0,000 415 | 102,3 | 0,000 515 | 107,3 | 0,000 590 | 112,3 |
| | 9 | 160 | 0,000 315 | 117,3 | 0,000 390 | 132,3 | 0,000 465 | 142,3 |
| | 10 | 187 | 0,000 215 | 152,3 | 0,000 290 | 167,3 | 0,000 540 | 177,3 |
| | 11 | 216 | 0,000 140 | 212,3 | 0,000 240 | 217,3 | 0,000 415 | 217,3 |
| | 12 | 247 | 0,000 190 | 272,3 | 0,000 265 | 272,3 | 0,000 490 | 257,3 |

**Table A.3** (*continued*)

| Year | Month | $L_S$ (°) | $C_R \times A/m = 0{,}04$ m²/kg | | $C_R \times A/m = 0{,}05$ m²/kg | | $C_R \times A/m = 0{,}06$ m²/kg | |
|---|---|---|---|---|---|---|---|---|
| | | | $e$ | $\omega + \Omega$ | $e$ | $\omega + \Omega$ | $e$ | $\omega + \Omega$ |
| 2021 | 1 | 279 | 0,000 240 | 312,3 | 0,000 340 | 302,3 | 0,000 465 | 297,3 |
| | 2 | 312 | 0,000 365 | 337,3 | 0,000 465 | 337,3 | 0,000 540 | 332,3 |
| | 3 | 342 | 0,000 465 | 12,3 | 0,000 565 | 7,3 | 0,000 640 | 2,3 |
| | 4 | 10 | 0,000 565 | 32,3 | 0,000 690 | 32,3 | 0,000 790 | 27,3 |
| | 5 | 38 | 0,000 665 | 52,3 | 0,000 765 | 52,3 | 0,000 890 | 47,3 |
| | 6 | 69 | 0,000 715 | 72,3 | 0,000 840 | 72,3 | 0,000 890 | 72,3 |
| | 7 | 100 | 0,000 665 | 92,3 | 0,000 765 | 92,3 | 0,000 890 | 92,3 |
| | 8 | 131 | 0,000 565 | 112,3 | 0,000 640 | 117,3 | 0,000 765 | 117,3 |
| | 9 | 160 | 0,000 440 | 132,3 | 0,000 540 | 137,3 | 0,000 640 | 142,3 |
| | 10 | 187 | 0,000 315 | 157,3 | 0,000 390 | 162,3 | 0,000 490 | 167,3 |
| | 11 | 216 | 0,000 165 | 182,3 | 0,000 265 | 197,3 | 0,000 390 | 197,3 |
| | 12 | 247 | 0,000 065 | 242,3 | 0,000 190 | 247,3 | 0,000 290 | 247,3 |
| 2022 | 1 | 280 | 0,000 165 | 342,3 | 0,000 215 | 312,3 | 0,000 340 | 297,3 |
| | 2 | 313 | 0,000 265 | 12,3 | 0,000 315 | 357,3 | 0,000 390 | 342,3 |
| | 3 | 341 | 0,000 390 | 27,3 | 0,000 515 | 22,3 | 0,000 540 | 12,3 |
| | 4 | 10 | 0,000 515 | 47,3 | 0,000 590 | 42,3 | 0,000 690 | 37,3 |
| | 5 | 38 | 0,000 565 | 62,3 | 0,000 665 | 62,3 | 0,000 765 | 57,3 |
| | 6 | 68 | 0,000 590 | 82,3 | 0,000 740 | 77,3 | 0,000 840 | 77,3 |
| | 7 | 99 | 0,000 615 | 97,3 | 0,000 715 | 97,3 | 0,000 840 | 97,3 |
| | 8 | 131 | 0,000 640 | 112,3 | 0,000 740 | 112,3 | 0,000 815 | 117,3 |
| | 9 | 160 | 0,000 590 | 132,3 | 0,000 715 | 132,3 | 0,000 765 | 142,3 |
| | 10 | 187 | 0,000 490 | 152,3 | 0,000 590 | 157,3 | 0,000 690 | 162,3 |
| | 11 | 216 | 0,000 365 | 182,3 | 0,000 490 | 192,3 | 0,000 590 | 197,3 |
| | 12 | 246 | 0,000 240 | 217,3 | 0,000 365 | 227,3 | 0,000 465 | 232,3 |
| 2023 | 1 | 279 | 0,000 165 | 272,3 | 0,000 290 | 272,3 | 0,000 390 | 277,3 |
| | 2 | 313 | 0,000 190 | 332,3 | 0,000 290 | 327,3 | 0,000 390 | 322,3 |
| | 3 | 341 | 0,000 265 | 7,3 | 0,000 390 | 2,3 | 0,000 490 | 2,3 |
| | 4 | 10 | 0,000 415 | 42,3 | 0,000 515 | 37,3 | 0,000 565 | 32,3 |
| | 5 | 37 | 0,000 540 | 67,3 | 0,000 640 | 62,3 | 0,000 740 | 57,3 |
| | 6 | 68 | 0,000 615 | 87,3 | 0,000 715 | 87,3 | 0,000 815 | 87,3 |
| | 7 | 99 | 0,000 590 | 107,3 | 0,000 715 | 107,3 | 0,000 865 | 102,3 |
| | 8 | 130 | 0,000 590 | 122,3 | 0,000 690 | 122,3 | 0,000 890 | 127,3 |
| | 9 | 159 | 0,000 540 | 147,3 | 0,000 640 | 147,3 | 0,000 740 | 147,3 |
| | 10 | 186 | 0,000 490 | 172,3 | 0,000 615 | 177,3 | 0,000 690 | 177,3 |
| | 11 | 215 | 0,000 490 | 202,3 | 0,000 590 | 207,3 | 0,000 690 | 207,3 |
| | 12 | 246 | 0,000 440 | 227,3 | 0,000 515 | 232,3 | 0,000 590 | 232,3 |

**Table A.3** (*continued*)

| Year | Month | $L_S$ (°) | $C_R \times A/m$ = 0,04 m²/kg | | $C_R \times A/m$ = 0,05 m²/kg | | $C_R \times A/m$ = 0,06 m²/kg | |
|---|---|---|---|---|---|---|---|---|
| | | | $e$ | $\omega + \Omega$ | $e$ | $\omega + \Omega$ | $e$ | $\omega + \Omega$ |
| 2024 | 1 | 279 | 0,000 340 | 257,3 | 0,000 440 | 262,3 | 0,000 540 | 267,3 |
| | 2 | 312 | 0,000 240 | 307,3 | 0,000 340 | 307,3 | 0,000 465 | 302,3 |
| | 3 | 342 | 0,000 215 | 347,3 | 0,000 315 | 347,3 | 0,000 440 | 347,3 |
| | 4 | 10 | 0,000 290 | 32,3 | 0,000 390 | 27,3 | 0,000 490 | 22,3 |
| | 5 | 38 | 0,000 390 | 62,3 | 0,000 465 | 57,3 | 0,000 565 | 57,3 |
| | 6 | 69 | 0,000 440 | 92,3 | 0,000 515 | 87,3 | 0,000 665 | 87,3 |
| | 7 | 100 | 0,000 440 | 122,3 | 0,000 565 | 117,3 | 0,000 690 | 112,3 |
| | 8 | 131 | 0,000 465 | 152,3 | 0,000 565 | 147,3 | 0,000 665 | 142,3 |
| | 9 | 160 | 0,000 465 | 172,3 | 0,000 590 | 172,3 | 0,000 665 | 167,3 |
| | 10 | 187 | 0,000 490 | 192,3 | 0,000 615 | 192,3 | 0,000 715 | 192,3 |
| | 11 | 216 | 0,000 490 | 217,3 | 0,000 615 | 217,3 | 0,000 715 | 217,3 |
| | 12 | 247 | 0,000 440 | 237,3 | 0,000 540 | 242,3 | 0,000 640 | 242,3 |
| 2025 | 1 | 279 | 0,000 415 | 257,3 | 0,000 540 | 262,3 | 0,000 615 | 267,3 |
| | 2 | 312 | 0,000 390 | 282,3 | 0,000 490 | 287,3 | 0,000 590 | 292,3 |
| | 3 | 342 | 0,000 290 | 307,3 | 0,000 390 | 312,3 | 0,000 465 | 322,3 |
| | 4 | 10 | 0,000 240 | 342,3 | 0,000 315 | 347,3 | 0,000 415 | 357,3 |
| | 5 | 38 | 0,000 165 | 32,3 | 0,000 265 | 37,3 | 0,000 365 | 37,3 |
| | 6 | 69 | 0,000 215 | 77,3 | 0,000 315 | 77,3 | 0,000 440 | 77,3 |
| | 7 | 100 | 0,000 290 | 117,3 | 0,000 465 | 112,3 | 0,000 515 | 112,3 |
| | 8 | 131 | 0,000 390 | 147,3 | 0,000 490 | 147,3 | 0,000 590 | 147,3 |
| | 9 | 160 | 0,000 465 | 177,3 | 0,000 565 | 177,3 | 0,000 665 | 172,3 |
| | 10 | 187 | 0,000 540 | 202,3 | 0,000 615 | 202,3 | 0,000 740 | 197,3 |
| | 11 | 216 | 0,000 640 | 227,3 | 0,000 765 | 227,3 | 0,000 890 | 227,3 |
| | 12 | 247 | 0,000 640 | 247,3 | 0,000 740 | 247,3 | 0,000 840 | 247,3 |

# Annex B
(informative)

# Optimal manoeuvre sequences

## B.1 General

Two types of manoeuvre sequences are suggested depending on whether the orbit perigee is optimal near-sun-pointing at the end of the spacecraft's operational life. Actual planning should consider mission constraints and uncertainties in estimating propellant usage.

The two main criteria for the manoeuvre sequence planning are the following:

a) ensuring sun-pointing or keeping final orbit eccentricity small (less than 0,005);

b) ensuring all on-board energy sources are depleted or passivated at the end of manoeuvres.

Clauses B.2 to B.4 illustrate the two types of manoeuvre sequences for impulsive burns with chemical propulsion systems. Clause B.5 discusses the two types of manoeuvre sequences for spacecraft utilizing low-thrust propulsion systems.

## B.2 Type A manoeuvre sequence

The initial perigee is already in the optimal direction, near-sun-pointing. Assuming there is an initial eccentricity of 0,000 5 and a target perigee of 300 km above GEO, the following actions should be taken:

a) perform the first burn at apogee to raise the perigee to GEO plus 200 km ($\Delta V = 4{,}0$ m/s);

b) perform a new orbit determination two orbits later;

c) perform the second burn at the new apogee to raise the perigee to GEO plus 300 km ($\Delta V = 5{,}0$ m/s);

d) perform a new orbit determination two orbits later;

e) perform the third burn at the new apogee to raise the perigee to GEO plus 250 km ($\Delta V = 0{,}9$ m/s and $e = 0{,}000\,589$);

f) perform a new orbit determination two orbits later;

g) perform the fourth burn at perigee to raise the apogee to GEO plus 350 km, if propellant is available ($\Delta V = 0{,}9$ m/s and $e = 0{,}001\,18$);

h) perform a new orbit determination 1,5 orbits later;

i) perform the fifth burn at apogee to raise the perigee to GEO plus 300 km ($\Delta V = 0{,}9$ m/s and $e = 0{,}000\,588$);

j) perform a new orbit determination two orbits later;

k) perform the sixth burn at apogee to raise the perigee to 325 km, if adequate propellant is available ($\Delta V = 0{,}45$ m/s and $e = 0{,}000\,294$);

l) continue to raise the perigee and apogee by about 25 km or less for each additional burn until propellant tanks are empty, and keep the perigee sun-pointing as shown for burns 7 and 8 in Table B.1; the last few burns should be small and well planned such that the final eccentricity vector is as close to the optimal vector as possible (see Annex C).

**Table B.1 — Orbit conditions and $\Delta V$ consumed after each Type A burn**

| Burn | Perigee height above GEO km | Apogee height above GEO km | Accumulated longitude drift ° west | $e$ | $\Delta V$ m/s | Accumulated $\Delta V$ m/s | Sun-pointing? |
|---|---|---|---|---|---|---|---|
| 1 | 21 | 200 | 0 | 0,002 120 | 4,0 | 4,0 | No |
| 2 | 200 | 300 | 3,2 | 0,001 170 | 5,0 | 9,0 | Yes |
| 3 | 250 | 300 | 11,2 | 0,000 589 | 0,9 | 9,9 | Yes |
| 4 | 250 | 350 | 20,0 | 0,001 180 | 0,9 | 10,8 | Yes |
| 5[a] | 300 | 350 | 27,6 | 0,000 588 | 0,9 | 11,7 | Yes |
| 6 | 325 | 350 | 35,9 | 0,000 294 | 0,45 | 12,15 | Yes |
| 7 | 325 | 375 | 44,5 | 0,000 592 | 0,45 | 12,6 | Yes |
| 8 | 350 | 375 | 55,6 | 0,000 296 | 0,45 | 13,05 | Yes |

[a] The minimum perigee increase, $\Delta H$, computed by Equation (1), can usually be satisfied after the fifth burn. The remaining burns are used to increase altitude until the propellant is exhausted (the accumulated $\Delta V$ is 13,05 m/s, assumed total $\Delta V$ remaining for orbit disposal).

The actual manoeuvre sequence should consider the ground-station-viewing constraint as the satellite is gradually drifting westward as shown in the fourth column of Table B.1. It may be two to three months before the last two to three burns (burns 6 to 8) can be performed. The estimated propellant mass to achieve a minimum perigee increase of 280 km is about 8 kg for a 2 000 kg spacecraft with a chemical propulsion system ($I_{sp} = 300$ s).

## B.3 Type B manoeuvre sequence

The initial perigee is not along the optimal direction for near-sun-pointing. When the initial perigee is not sun-pointing, the long-term eccentricity variation will be more pronounced and the minimum perigee altitude will be lower than the desired value of 300 km. The standard re-orbit strategy is to execute the first two to three burns away from perigee or apogee to change the argument of perigee or the eccentricity vector. The change can be achieved without additional propellant or burns. Figure B.1 gives an example of induced change in argument of perigee versus the burn location on the orbit.

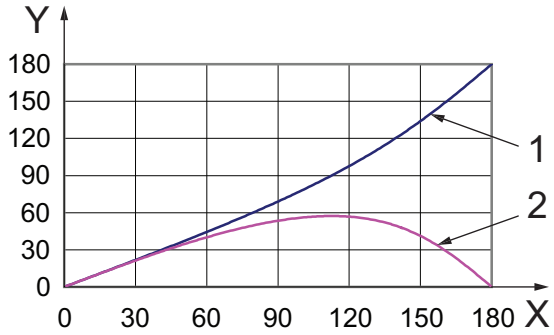


**Key**

X burn location (true anomaly), in degrees

Y change in argument of perigee, in degrees

1 exact solution

2 Equations (B.1) and (B.2)

**Figure B.1 — Induced change in argument of perigee versus burn location**

The example assumes an initial eccentricity of 0,000 5 and the $\Delta V$ as 2,0 m/s. This burn will also raise the semi-major axis by the desired amount, approximately 110 km. The top curve is computed from equations based on closed-form orbit relations to be discussed in Annex C. The bottom curve is computed from simplified linear relations as follows:

$$\Delta e = \frac{\Delta a}{a} \times \cos v \tag{B.1}$$

$$e\Delta\omega = \frac{\Delta a}{a} \times \sin v \tag{B.2}$$

where

$\Delta e$ is the induced change in eccentricity;

$\Delta\omega$ is the induced change in argument of perigee;

$\Delta a$ is the planned increase in mean orbit altitude or semi-major axis;

$v$ is the true anomaly where a single burn is executed.

The eccentricity in front of $\Delta\omega$ on the left-hand side of Equation (B.2) is the new eccentricity after the burn. Figure B.1 shows that the simplified relations for determining the induced change in argument of perigee give good approximations when the burn location (true anomaly or central angle from perigee) is less than 90°. Equations (B.1) and (B.2) are useful in the initial design of the Type B manoeuvre sequence for orbits whose perigees are not sun-pointing.

Figure B.2 shows the corresponding change in eccentricity. The approximate relation [Equation (B.1)] is good for eccentricity computation when the true anomaly is less than 40°.

When the perigee becomes sun-pointing after the first two or three burns, the remaining burn sequences should follow the Type A manoeuvre sequence.

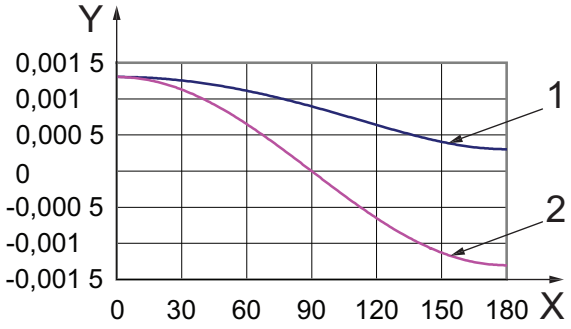


**Key**

X burn location (true anomaly), in degrees
Y change in eccentricity
1 exact solution
2 Equation (B.1)

**Figure B.2 — Induced change in eccentricity versus burn location** ($e_0 = 0{,}000\ 5$; $\Delta V = 2{,}0$ m/s)

## B.4 Sample manoeuvre sequence

The following sample manoeuvre sequence assumes a 70° difference between the initial perigee and the sun vector (the sun is 70° east of the perigee vector):

a) perform the first burn at 60° past perigee or when true anomaly equals 60°, with a $\Delta V$ of 2,0 m/s along the in-track direction to raise orbit altitude;

b) perform an orbit determination one or two orbits later; the new orbit should be $a = 42\ 220{,}86$ km, $e = 0{,}001\ 613$, same inclination and RAAN, and argument of perigee advanced by 44,42°;

c) perform the second burn at 56° past the new perigee, with a $\Delta V$ of 2,0 m/s along the in-track direction;

d) perform an orbit determination one or two orbits later; the new orbit after the second burn should be sun-pointing with $a = 42\ 275{,}96$ km, $e = 0{,}002\ 584$, and argument of perigee advanced by another 25°;

e) perform the third burn at the new apogee to raise the perigee to GEO plus 250 km ($\Delta V = 4{,}52$ m/s and $e = 0{,}000\ 362$);

f) perform an orbit determination two orbits later;

g) perform the fourth burn at the new apogee to raise the perigee to GEO plus 325 km ($\Delta V = 1{,}91$ m/s and $e = 0{,}000\ 883\ 3$);

h) perform an orbit determination two orbits later;

i) perform the fifth burn at the apogee to raise the perigee to GEO plus 300 km ($\Delta V = 0{,}9$ m/s and $e = 0{,}000\ 294$);

j) perform an orbit determination two orbits later;

k) perform the sixth burn at the perigee to raise the apogee by 50 km if propellant is available ($\Delta V = 0{,}9$ m/s and $e = 0{,}000\ 872$);

l) repeat B.4 h) and B.4 i) to raise the perigee by 25 km ($\Delta V = 0{,}45$ m/s) after each additional burn, and continue until propellant tanks are empty as illustrated in Table B.2.

**Table B.2 — Orbit conditions and $\Delta V$ consumed after each Type B burn**

| Burn | Perigee height above GEO km | Apogee height above GEO km | Accumulated longitude drift ° west | $e$ | $\Delta V$ m/s | Accumulated $\Delta V$ m/s | Sun-pointing? |
|---|---|---|---|---|---|---|---|
| 1 | 13 | 123 | 0 | 0,001 613 | 2,0 | 2,0 | No |
| 2 | 1 | 219 | 1,74 | 0,002 584 | 2,0 | 4,0 | Yes |
| 3 | 219 | 250 | 4,55 | 0,000 362 | 4,52 | 8,52 | No |
| 4 | 250 | 325 | 10,5 | 0,000 893 | 1,91 | 10,43 | Yes |
| 5 | 300 | 325 | 18,0 | 0,000 294 | 0,9 | 11,33 | Yes |
| 6 | 300 | 375 | 26,0 | 0,000 872 | 0,9 | 12,23 | Yes |
| 7 | 325 | 375 | 34,6 | 0,000 592 | 0,45 | 12,68 | Yes |
| 8 | 350 | 375 | 43,5 | 0,000 296 | 0,45 | 13,13 | Yes |

The actual manoeuvre sequence should consider the ground-station-viewing constraint as the satellite is gradually drifting westward as shown in the fourth column of Table B.1. It may be two to three months before the last two to three burns (burns 6 to 8) can be performed. The estimated propellant mass to achieve a minimum perigee increase of 280 km is about 8 kg for a 2 000 kg spacecraft with a chemical propulsion system ($I_{sp}$ = 300 sec).

## B.5 Manoeuvre sequence for low-thrust propulsion

For simplified illustration, we assume that a near-circular geostationary orbit is gradually pushed into the desired disposal orbit using a continuous and constant low-thrust propulsion along the velocity direction. The changes in semi-major axis and the eccentricity vector may be understood through the following set of Gaussian form of equations of motion.

$$\frac{\mathrm{d}a}{\mathrm{d}t} = \frac{2aF}{V} \tag{B.3}$$

$$\frac{\mathrm{d}h}{\mathrm{d}t} = \frac{2F\sin L}{V} \tag{B.4}$$

$$\frac{\mathrm{d}k}{\mathrm{d}t} = \frac{2F\cos L}{V} \tag{B.5}$$

$$\frac{\mathrm{d}L}{\mathrm{d}t} = n \tag{B.6}$$

where

$h = e\cos(\omega + \Omega)$;

$k = e\sin(\omega + \Omega)$;

$L = M + \omega + \Omega$;

$a$ is the semi-major axis;

$F$ is the constant acceleration along the velocity direction;

$V$ is the magnitude of the velocity;

$n$ is the orbit mean motion;

$M$ is the mean anomaly.

Equations (B.3) to (B.6) can be integrated by assuming constant $a$ and $V$ for a small increase in mean orbit altitude, e.g. $\Delta H = 280$ km, as follows:

$$\Delta a = \frac{2aF\Delta t}{V} \tag{B.7}$$

$$\Delta h = \frac{2F\left(\cos L_0 - \cos L_1\right)}{Vn} \tag{B.8}$$

$$\Delta k = \frac{2F\left(\sin L_1 - \sin L_0\right)}{Vn} \tag{B.9}$$

$$L_1 = L_0 + n\Delta t \tag{B.10}$$

The time required for the low-thrust propulsion to achieve the desired altitude increase can be determined from Equations (B.3) to (B.5), or from Equation (B.11):

$$\Delta t = \frac{\Delta HV}{2aF} \tag{B.11}$$

For the Type A manoeuvre sequence, no change in eccentricity vector for retaining sun-pointing geometry is required. Therefore, $\Delta t > \frac{\Delta HV}{2aF}$ and $L_1 \approx L_0$.

For the Type B manoeuvre sequence, the time of action of the low-thrust propulsion should be such that the desired altitude increase is reached and the final eccentricity vector is sun-pointing. For example, a GEO spacecraft is equipped with the xenon ion propulsion system (XIPS) designed by the Boeing Company. The estimated thrust level is about 80 mN and the specific impulse ($I_{sp}$) is 3 400 s. Assuming the mass of the spacecraft at end-of-life is 2 000 kg, the estimated acceleration generated from the XIPS is approximately $(0{,}4 \times 10^{-4})$ m/sec$^2$. From Equation (B.11), the time required to reach 280 km above GEO is 2 956 days. In order to ensure sun-pointing, the propulsion should continue to act for an additional three days or three orbit revolutions to the point where $L_1$ is equal or close to $L_0$. The required propellant mass for this transfer is about 0,7 kg (which is less than one-tenth of the mass using chemical propulsion).

In actual application, the low-thrust propulsion systems of a particular spacecraft can be rather complex with burn constraints. A detailed manoeuvre sequence should be outlined to achieve the required minimum perigee altitude increase and the desired sun-pointing geometry. A description should be included of the method to be used to monitor the remaining propellant and to estimate the effective thrust level.

# Annex C
(informative)

# Example calculations

## C.1 Closed-form equations for computing off-perigee burn locations

When a re-orbit burn is applied at a location away from perigee or apogee, changes in argument of perigee and eccentricity occur. The magnitude and direction of the changes depend on the burn vector and location of the burn.

In this application, the single-burn vector is assumed to be along the in-track direction or perpendicular to the radial direction and the burn is assumed to be impulsive. The computation starts with a given $\Delta V$ applied at a given location on the orbit or true anomaly $v$. The following Keplerian relations will lead to the induced eccentricity and argument of perigee.

If the total orbital velocity after the burn, $V$, is calculated from

$$V = V_0 + \Delta V \tag{C.1}$$

where $V_0$ is the orbital velocity before the burn, then from the *vis-viva* integral, the new semi-major axis, $a$, is computed as shown in Equation (C.2) after the $\Delta V$ is applied at a given true anomaly $v$:

$$a = \frac{1}{2/r - V^2/\mu} \tag{C.2}$$

where

$r$ is the radius of the orbit at the time of burn;

$\mu$ is the gravitational constant for the Earth.

Assuming that the $\Delta V$ is along the in-track direction and the velocity component in the radial direction is not affected, one Keplerian relation gives Equations (C.3) and (C.4):

$$e\cos v = \frac{p}{r} - 1 = \frac{a\left(1-e^2\right)}{r} - 1 \tag{C.3}$$

$$e\sin v = (\mu / p_0)^{1/2} \times (p/\mu)^{1/2} \times e_0 \sin v_0 = (p/p_0)^{1/2} e_0 \sin v_0 \tag{C.4}$$

where

$$p = a\left(1-e^2\right) \tag{C.5}$$

$$p_0 = a_0\left(1-{e_0}^2\right) \tag{C.6}$$

and $p_0$, $a_0$ and $e_0$ are the elements before the burn.

Equations (C.3) and (C.4) can then be used to calculate $e$ and $v$ by iteration, through Equations (C.7) and (C.8):

$$e^2 = (e\sin v)^2 + (e\cos v)^2 \tag{C.7}$$

and

$$v = \tan^{-1}\left(\frac{e\sin v}{e\cos v}\right) \tag{C.8}$$

After knowing the true anomaly, $v$, the new value of argument of perigee is as calculated in Equation (C.9):

$$\omega = v_0 + \omega_0 - v \tag{C.9}$$

With Equations (C.1) to (C.9), the burn location, $v_0$, can be determined by iteration.

## C.2 Sample 100-year histories of sun-pointing disposal orbits

A sun-pointing geometry is selected by assuming an epoch of 2018-07-01. Figure C.1 illustrates the sun-pointing geometry of this example. A midnight-pointing perigee would be achieved for the same initial orbital elements by changing the epoch to 2018-01-01.

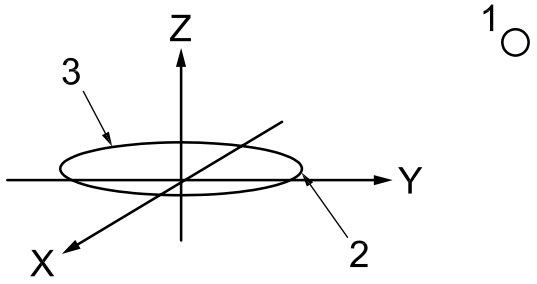


**Key**

| | |
|---|---|
| X, Y, Z | Earth-centred Cartesian coordinates |
| 1 | sun |
| 2 | perigee of disposal orbit |
| 3 | disposal orbit |

**Figure C.1 — Sun-pointing geometry with 2018-07-01 epoch**

The sample orbital elements of a GEO disposal orbit for 100-year integration are determined from the assumed initial eccentricity of 0,000 5 with $A/m = 0{,}035$ m$^2$/kg and $C_R = 1{,}3$. The recommended altitude increase, $\Delta V$, expressed in km, is

$$\Delta H = 235 + (1\,000 \times C_R \times A/m) = 235 + (1\,000 \times 1{,}3 \times 0{,}035) = 280{,}5 \text{ km} \tag{C.10}$$

The corresponding semi-major axis is 42 467,6 km, $e = 0{,}000\,5$, $i = 0{,}1°$, $\Omega = 90°$, $\omega = 0°$, and $M = 0°$. A high-precision N-body numerical integration tool was employed to generate all the long-term orbit results presented in Figures C.2 to C.7. The perturbing forces included are Earth's gravitational harmonics (6 by 6 EGM96), lunisolar attractions and solar radiation pressure.

Figure C.2 shows the sun-pointing perigee height history of the 100-year integration. The perigee height history of such orbit is well behaved, with the perigee never below GEO plus 250 km. However, when the perigee is pointing to the local midnight, a much larger oscillation in perigee height is found in the 100-year

integration (see Figure C.3). The minimum perigee height above GEO is approaching 200 km. This finding suggests that the re-orbit insertion should be performed with perigee pointing to the sun. A long-period perigee height variation with a period of about 10,5 years, caused by sun/moon attractions, is apparent in these two cases (see Figures C.2 and C.3), as well as the other 100-year eccentricity histories.

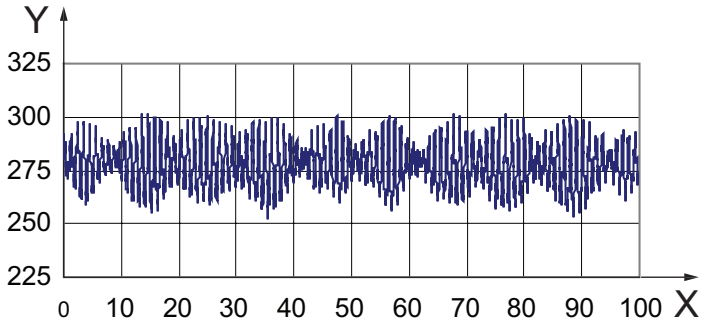


**Key**

X years after 2018

Y perigee above GEO, in km

**Figure C.2 — 100-year perigee history (sun-pointing)**

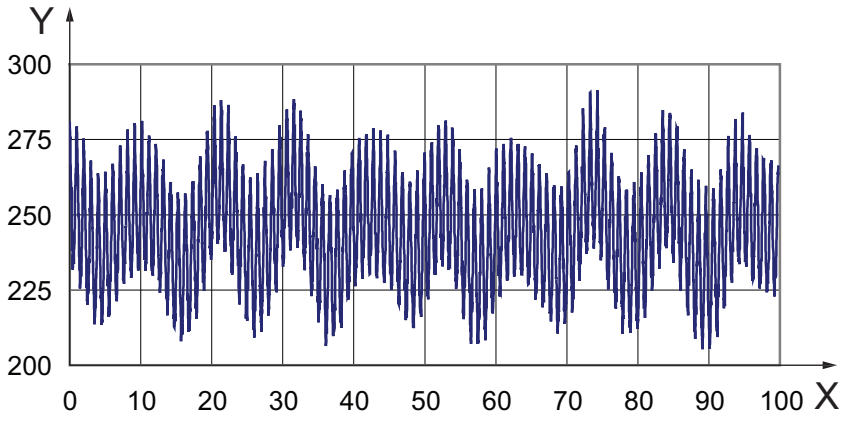


**Key**

X years after 2018

Y perigee above GEO, in km

**Figure C.3 — 100-year perigee history (pointing to midnight)**

Several cases of 100-year integration were repeated to study the sensitivity of perigee height to epoch. The initial orbit elements are the same as before for each case at 07-01 or 01-01 of each epoch year. In each 100-year integration, only the minimum perigee height above GEO is recorded and plotted, as in Figure C.4. The upper curve represents the minimum perigee height for the 07-01 epoch (sun-pointing), and the lower curve represents the minimum perigee height for the 01-01 epoch (perigee pointing to midnight). The epoch is varied from 2005-01-01 to 2025-07-01. Figure C.4 shows the sensitivity of minimum perigee height to epoch.

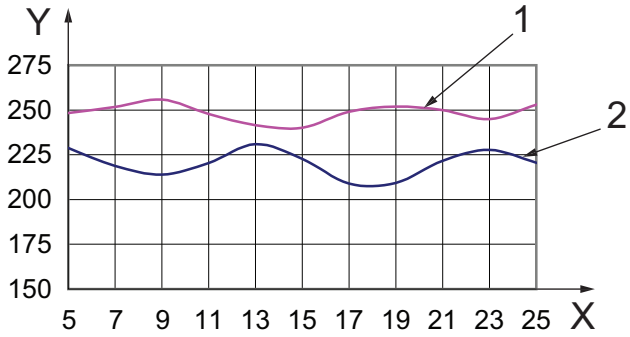


**Key**

X years after 2000
Y minimum perigee height above GEO, in km
1 epoch on 07-01
2 epoch on 01-01

**Figure C.4 — Minimum perigee height versus epoch**

To determine whether there is a seasonal variation, the 100-year integration only for the sun-pointing case (upper curve in Figure C.4) is repeated on the first day of each month for four selected years (2005, 2009, 2014 and 2018). Figure C.5 shows the seasonal variation of the minimum perigee heights. The four curves in Figure C.5 reveal another interesting fact: the peak of the seasonal variation changes to a valley about every 4 years, or one-quarter of the 18,6 year lunar cycle. The same trend can be seen in Figure C.4, where the peaks occur in summer (07-01) for 2009 and 2018.

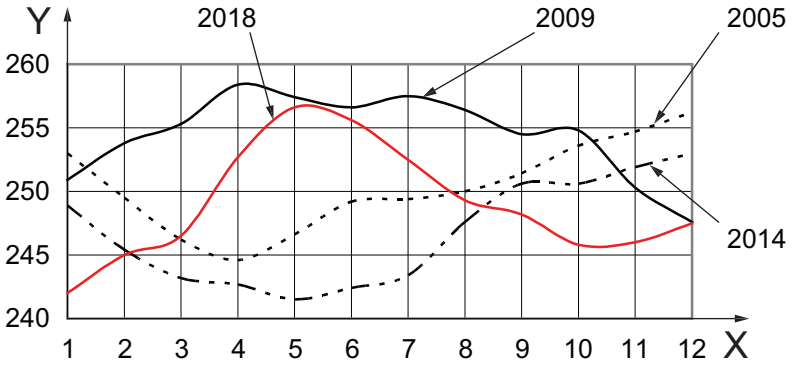


**Key**

X month of the year
Y minimum perigee height above GEO, in km

**Figure C.5 — Minimum perigee height versus month of the year**

This finding reveals that the recommended altitude increase (280,5 km) yields a minimum perigee of 250 km or higher for 100 years if the orbit insertion is performed near the peak season (Figures C.4 and C.5) following sun-pointing geometry. For example, if a disposal orbit manoeuvre sequence is to be planned in 2009, the best time for the re-orbit is some time in April, as indicated in Figure C.5.

When the perigee is pointing away from the sun or toward midnight, the minimum perigee height from the 100-year integration changes in a different way. Figure C.6 shows the minimum perigee height as a function of the combined angle, $(\omega + \Omega)$, for two epochs. On 07-01, the sun-pointing geometry occurs when $(\omega + \Omega) = 90°$. On 01-01, the sun-pointing geometry occurs when $(\omega + \Omega) = 270°$. The results show that the highest value of minimum perigee height occurs when the perigee is sun-pointing.

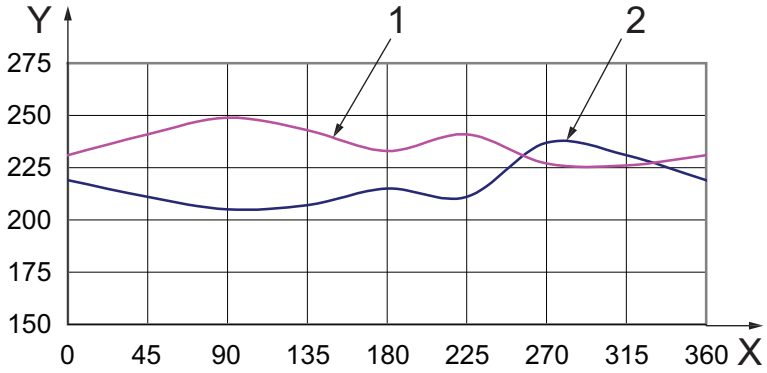


**Key**

X angle of RAAN plus argument of perigee, in degrees

Y minimum perigee height above GEO, in km

1 epoch on 07-01

2 epoch on 01-01

**Figure C.6 — Minimum perigee height versus** $(\omega + \Omega)$

Figure C.7 shows the minimum perigee height above GEO determined from 100-year integration versus the initial eccentricity of the disposal orbit. The same set of initial orbital elements is assumed with two epochs, 2018-07-01 and 2018-01-01. All the cases satisfy the initial perigee altitude increase, $\Delta H$, determined by Equation (C.10) (280,5 km).

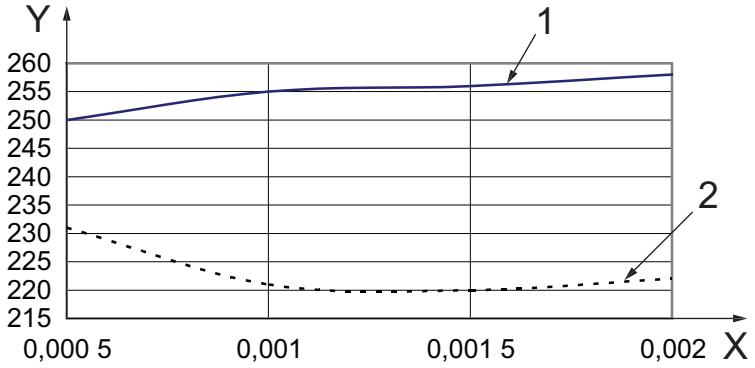


**Key**

X initial eccentricity

Y minimum perigee height above GEO, in km

1 sun-pointing

2 midnight-pointing

**Figure C.7 — Minimum perigee height above GEO versus initial eccentricity**

The results indicate that smaller eccentricity, at 0,000 5, tends to keep the minimum perigee higher, at 230 km, when the perigee is pointing to midnight (dashed curve in Figure C.7). The results also show that larger initial eccentricity actually increases the minimum perigee height if the sun-pointing geometry is followed (solid curve in Figure C.7). However, larger initial eccentricity with the same initial perigee altitude increase (280,5 km) requires more propellant, which is undesirable for mission operations. Figure C.8 gives an estimate of the $\Delta V$ requirement as a function of initial eccentricity of a GEO disposal orbit with an initial altitude increase of 280,5 km.

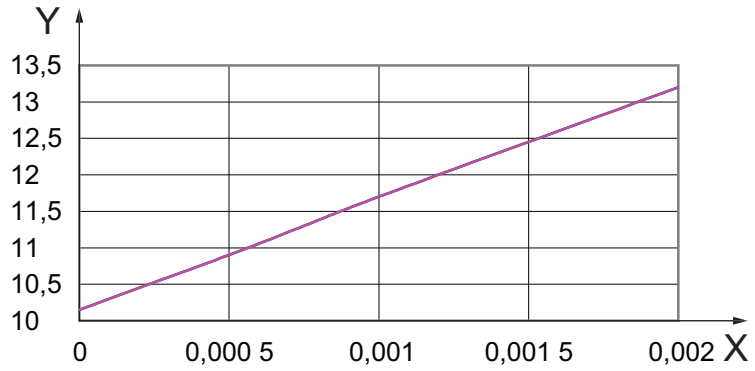


**Key**

X initial eccentricity

Y $\Delta V$ requirement, in m/sec

**Figure C.8 — $\Delta V$ required for re-orbit versus eccentricity**

As seen from the linear relation in Figure C.8, an initial eccentricity of 0,002 requires about 2,4 m/s or 22 % more $\Delta V$ than an eccentricity of 0,000 5 requires.

The uncertainties of the long-term prediction of perigee altitudes may be estimated from the uncertainties in predicting the semi-major axis and eccentricity. The major source of error in predicting the semi-major axis and eccentricity of a super-synchronous orbit comes from the uncertainty in modelling the solar radiation pressure that is proportional to the effective $A/m$ of the spacecraft. Because of the uncertainty in the attitude of an inactive spacecraft, it is difficult to estimate accurately the effective $A/m$. In the 100-year predictions presented here, a constant effective $A/m$ of 0,035 $m^2$/kg with a $C_R$ value of 1,3 is assumed for all cases. Numerical tests show that a 20 % decrease in $A/m$ will increase the minimum perigee height by about 5 km.

To summarize, the sample plots shown in Figures C.1 to C.7 illustrate that long-term eccentricity or perigee stability of GEO disposal orbits can be significantly improved by the following:

a) having the initial perigee pointing to the sun;

b) performing the re-orbit in the most favourable season of the year.

# Annex D
(informative)

# Disposal strategy and analysis for sample GEO satellite

Normally, at the end of its useful life, a satellite is moved to a higher orbit with a minimum perigee, ranging from 235 km to 300 km above GEO. Often the satellite is disposed of in a few manoeuvres. However, the satellite being moved may have an unknown amount of propellant or a questionable state of health. This implies that the vehicle could fail at any time and, therefore, relying upon a few large burns may not be the best way to get the largest clearance from the GEO belt over a long period.

Instead, a safer method of disposal is to target an optimal eccentricity and argument of perigee and try to conduct smaller burns in pairs approximately 12 h (or 36 h) apart. In this manner, the 100-year perigee altitude behaviour stays consistently higher than it otherwise would, possibly by as much as 40 km to 50 km for the same cost in $\Delta V$. This significantly reduces the risk of collision between the disposed satellite and other operational vehicles in GEO. A sample case for a GEO satellite is examined below to show the net effect of the proposed strategy.

The predisposal conditions for the sample satellite were eccentricity of 0,000 317, 7,7° inclination, 62,3° RAAN, 353° argument of perigee, ($C_R \times A/m$) of 0,037 4 $m^2$/kg, and an epoch of 2005-05-28. The satellite was assumed to be originally in GEO, with a final desired disposal orbit at least 300 km above GEO.

A mean element propagator was used to generate 100-year histories of the perigee altitude above GEO for a variety of initial conditions. The force models used were the 6 by 6 EGM96 gravity field, solar radiation pressure, and solar and lunar perturbations.

Sweeping over the entire range of argument of perigee, from 0° to 360°, for various eccentricities, and saving the minimum perigee altitude over 100 years from each run, produces the results shown in Figure D.1. Once again, the initial inclination and node were 7,7° and 62,3°, respectively, with a semi-major axis of 160 km above GEO. The argument of perigee increment was 5°; the eccentricity increment was $1 \times 10^{-4}$. For this sample case, the optimal argument of perigee was approximately 20°; the worst argument of perigee was at 200°. The sun-pointing strategy would imply an argument of perigee of about 5°; the true optimal point is thus somewhat different from the sun-pointing angle. Figure D.1 shows that the optimal point is strongly dependent upon the initial argument of perigee and weakly dependent upon the eccentricity. The difference between the highest and lowest minimum perigee altitude is over 50 km irrespective of the eccentricity, implying that targeting the optimal argument of perigee is very important to a successful disposal strategy.

Figure D.2 shows the dependency of minimum perigee altitude on eccentricity at the optimal argument of perigee of 20°. The same initial conditions were used as in Figure D.1, but a finer resolution in the eccentricity of $2{,}5 \times 10^{-5}$ was used to get a more accurate result. For this satellite, the preferred target eccentricity was about 0,000 590. The nominal sun-pointing strategy implies a target eccentricity of only 0,000 374 ($0{,}01 \times C_R \times A/m$). However, as will be demonstrated below, the solar and lunar perturbations contribute to the value of the eccentricity and the solar radiation pressure causes the higher target value.

The burns should be planned to keep the postburn eccentricity and argument of perigee as close to the target values as possible. From Figures D.1 and D.2, there is a tolerance of approximately +10° in the argument of perigee and +0,000 16 in eccentricity to maintain a minimum perigee altitude within 5 km of the maximum value. These are well within the targeting capabilities of GEO satellites.

NOTE These values apply only to the sample case as set forth here. Differing initial conditions, especially the node, epoch and solar radiation coefficient, will change the optimal values. As will be demonstrated below, the semi-major axis and inclination contribute little to the optimal values of the argument of perigee and eccentricity.

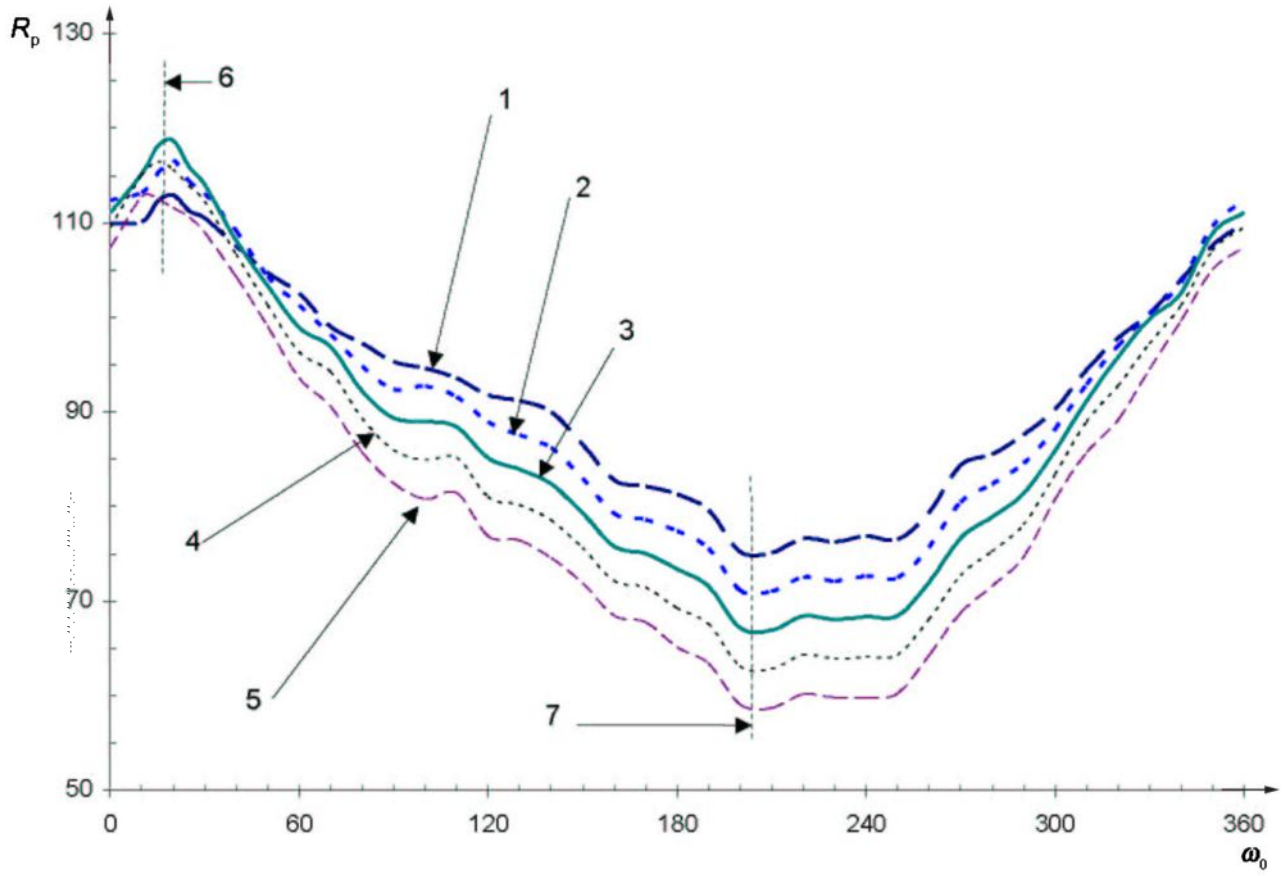


**Key**

$R_p$ minimum perigee altitude over 100 years, in km
$\omega_0$ initial argument of perigee
1 eccentricity of 0,000 39
2 eccentricity of 0,000 49
3 eccentricity of 0,000 59
4 eccentricity of 0,000 69
5 eccentricity of 0,000 79
6 optimal argument of perigee
7 worst argument of perigee

**Figure D.1 — Dependency of minimum perigee altitude on argument of perigee**

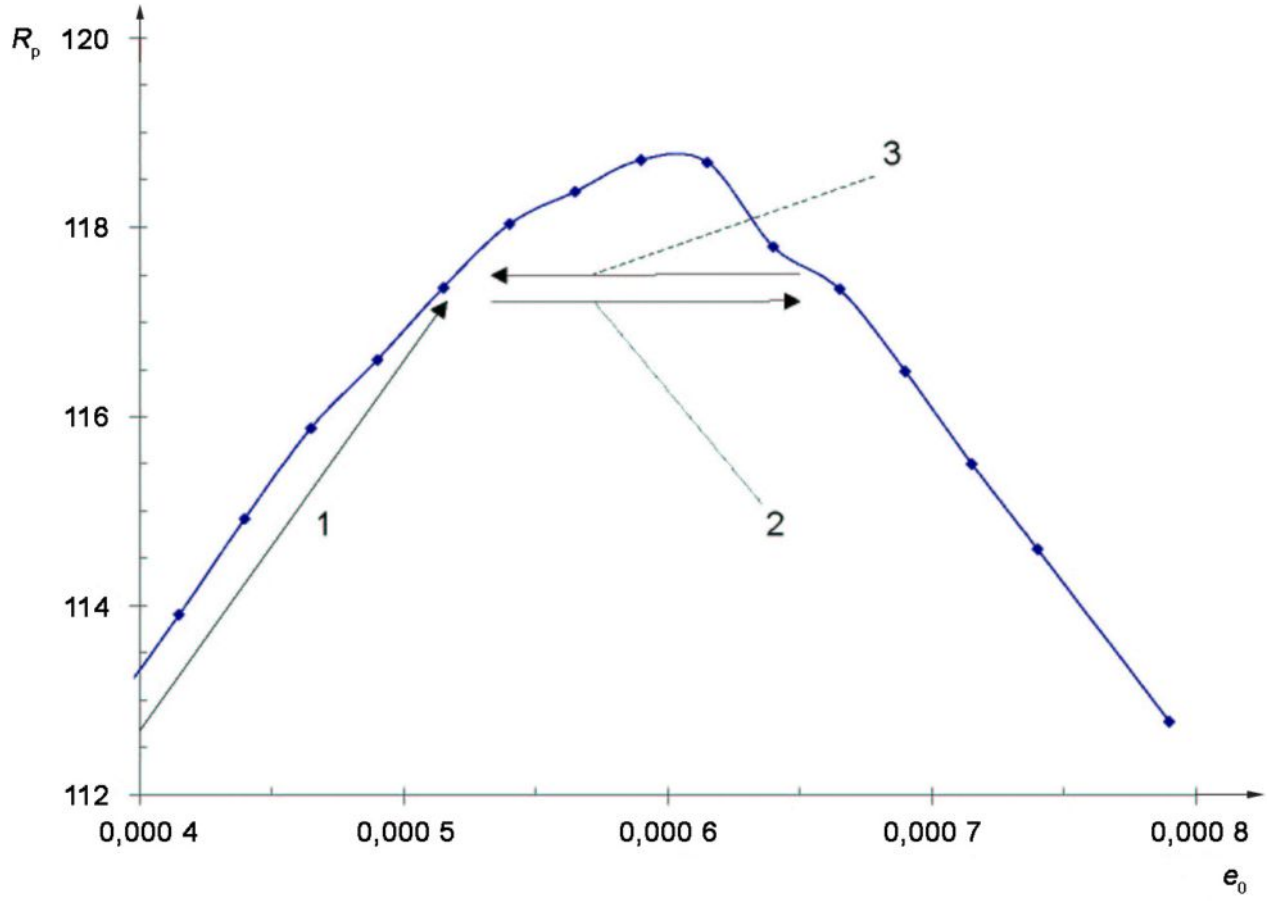


**Key**

$R_p$ minimum perigee altitude over 100 years, in km

$e_0$ initial eccentricity

1 initial burn

2 first burn of pair

3 second burn of pair

**Figure D.2 — Dependency of minimum perigee altitude on eccentricity**

As an example, burn profile is also shown in Figure D.2. The initial burn would be performed to increase the eccentricity from the predisposal value of 0,000 317 to 0,000 52 while moving the argument of perigee to within 10° of the target value of 20°. Then subsequent burns would take place in pairs. The first burn of the pair increases the altitude and raises the eccentricity to 0,000 65 while keeping the argument of perigee close to 20°. The second burn of the pair also raises the altitude but decreases the eccentricity back to 0,000 52 and so on until the desired change in altitude is accomplished. In essence, the satellite is manoeuvred incrementally up to the desired disposal altitude. If a failure occurs at any point, then the satellite is guaranteed of achieving the best possible clearance over the next 100 years.

Figure D.3 shows the dependency of the minimum perigee altitude over the next 100 years broken down by the type of perturbation for the optimal eccentricity of 0,000 590. The gravitational field alone (indicated by the empty circles in Figure D.3) does not contribute very much to the argument of perigee dependency; neither does the solar gravitation (shown as asterisks). Instead, the solar radiation pressure (squares) and the lunar perturbation (solid circles) act together to create the results for the combined perturbations (solid line). Note that for the solar radiation pressure, optimal argument of perigee is at about 5°, given the epoch of 2005-05-28 (solar longitude of 66°) and the initial RAAN of 62°, which implies that the orbit would be very near the sun-pointing orientation (argument of perigee plus RAAN equates to solar longitude). However, the presence

of the lunar perturbations causes the final optimal point to deviate from the ideal sun-pointing strategy. Additional runs performed at epochs four months and eight months later confirmed these results.

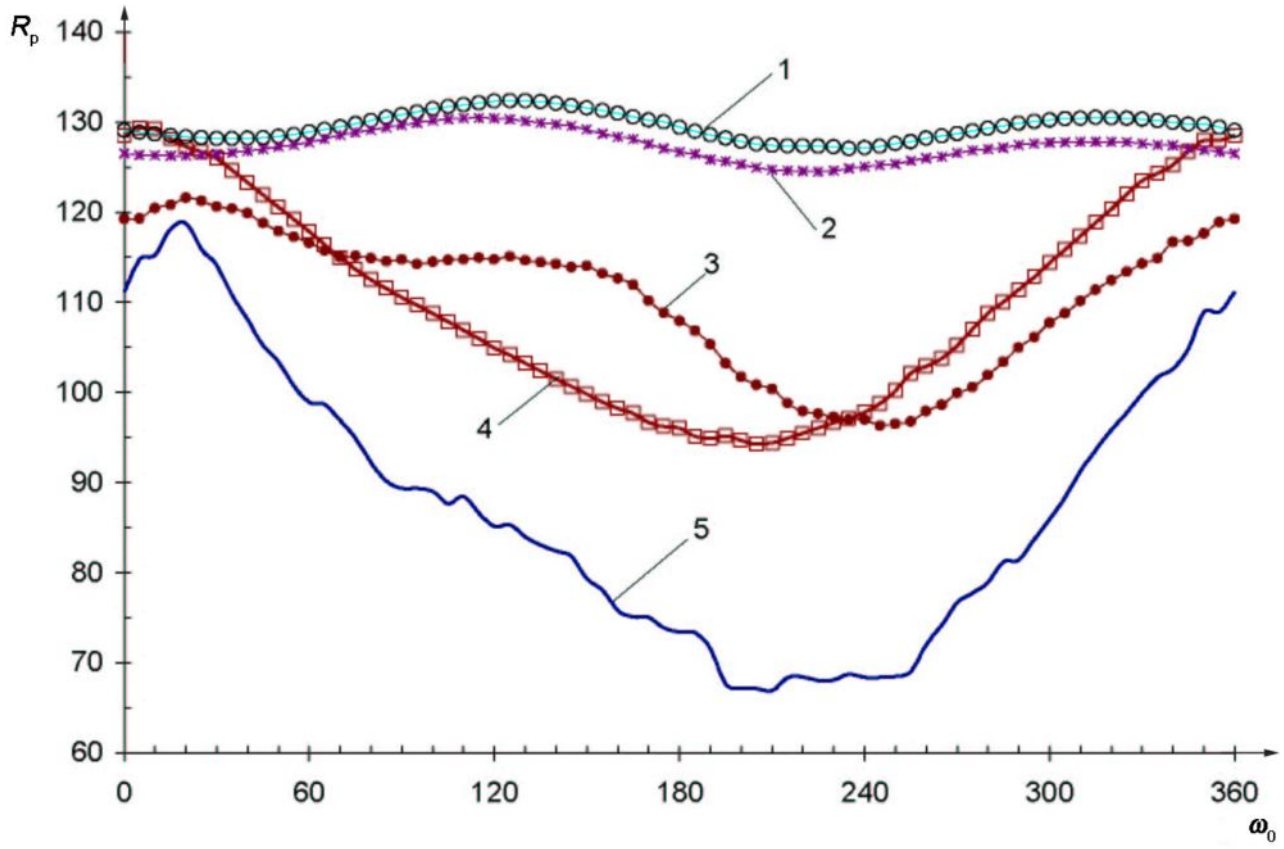


**Key**

$R_p$ minimum perigee altitude over 100 years, in km

$\omega_0$ initial argument of perigee

1 $6 \times 6$ gravity field only

2 $6 \times 6$ gravity field plus sun

3 $6 \times 6$ gravity field plus moon

4 $6 \times 6$ gravity field plus solar radiation pressure

5 $6 \times 6$ gravity field plus sun and moon plus solar radiation pressure

**Figure D.3 — Contribution of individual perturbations**

Once the optimal eccentricity and argument of perigee have been established, the question is how sensitive are the target values to changes in the semi-major axis (i.e. as the satellite moves higher during the manoeuvre sequence, do the optimal values change in any significant way?). Runs were performed to find the optimal argument of perigee and eccentricity for varying semi-major axes while keeping the node and epoch constant. This was also performed for varying inclinations to determine the sensitivity to that orbit parameter. Neither case produced a significant change in the optimal values. However, when the semi-major axis was precisely at GEO altitude, the optimal values were noticeably different ($e$ approximately 0,000 490 4 and $\omega$ approximately 60°). This is because the gravitational field harmonics were in resonance at GEO altitude. Still, once the satellite moved even slightly above GEO (approximately 50 km), the optimal eccentricity and argument of perigee settled down to consistent values.

After the initial burn is performed as shown in Figure D.1, how should the subsequent burn pairs be conducted? The usual assumption is to burn in pairs at perigee and apogee so as to keep the argument of perigee constant. However, Figure D.4 shows the effect of the timing of the burns in relation to each other.

This plot was generated by assuming a first burn at a certain location in the orbit and then trying the second burn at separate 1 h intervals over the next 24 h. The $x$-axis shows the hours past perigee of the first burn (24 h to one orbit at GEO so burns at both 0 h and 24 h are at perigee). There are two $y$-axes: the left-hand axis (solid diamonds) shows the subsequent minimum perigee altitude over the next 100 years for a given pair of burns, while the right-hand axis (open squares) shows the time of the second burn in relation to the first burn. The magnitude of the burns was 0,5 m/s.

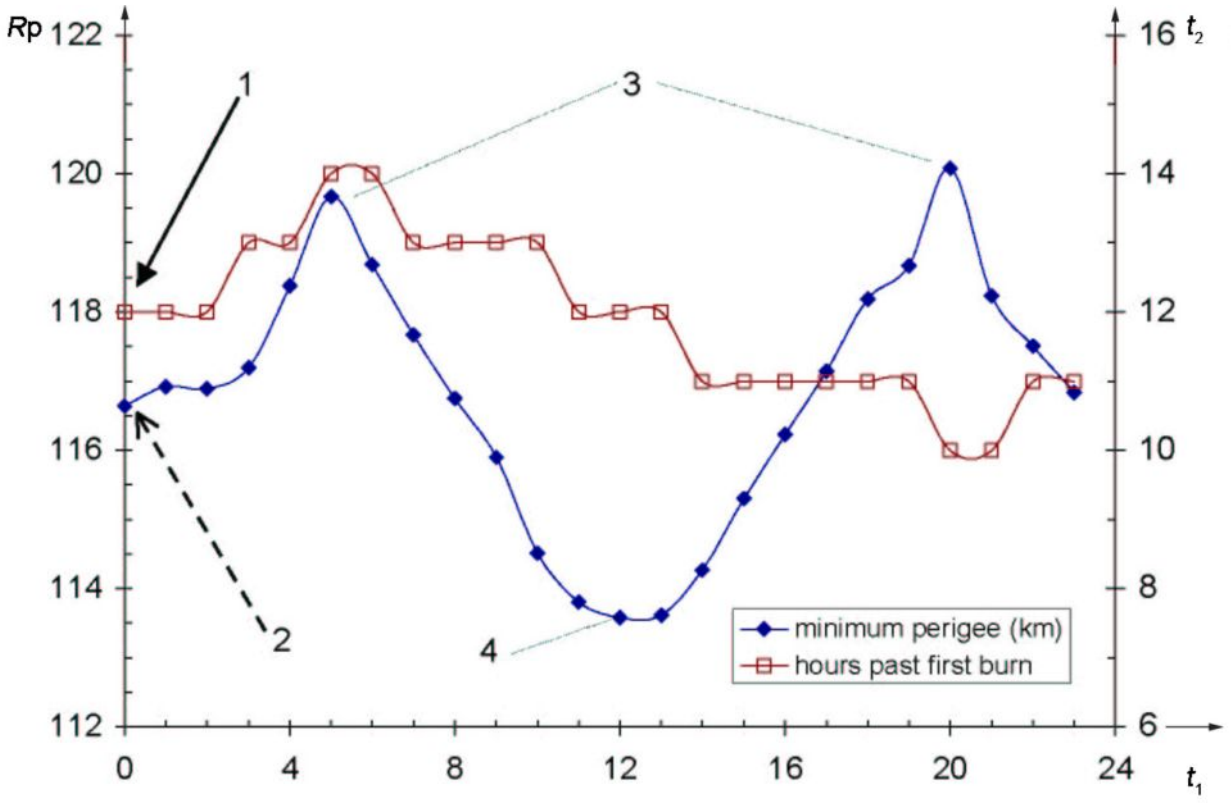


**Key**

$R_p$ minimum perigee altitude over 100 years, in km
$t_1$ hours past perigee for first burn in the pair
$t_2$ hours past the first burn when second burn occurs
1 hours past the first burn when second burn occurs for sample burn pair
2 highest minimum perigee for sample burn pair
3 best burn pairings
4 worst burn pairing

**Figure D.4 — Optimal locations in orbit for burn pair**

For example, if the first burn of the pair is performed at perigee (0 h), then 24 subsequent runs are performed at 1 h, 2 h, 3 h, etc., after perigee. The highest (best) minimum perigee of the 24 runs is saved. In this case, the highest minimum perigee occurred when the second burn was at 12 h past the first burn (this curve is denoted by the solid arrow and is associated with the right-hand $y$-axis) and yielded a perigee altitude of 116,6 km (this curve is denoted by the dashed arrow and is associated with the left-hand $y$-axis). As this plot shows, the best burn pairing does not occur at perigee/apogee but is actually almost 90° away from that location. The deviation, however, is not much: only about 6 km from peak to valley.

Conversely, Figure D.5 shows several sample cases denoting the two best solutions from Figure D.4 at 5 h and 20 h, along with the worst solution at 12 h and the perigee (0 h) solution. Here the variation is 30 km, peak to valley. The conclusion from these two figures is that, while there may be optimal times within a given

orbit to conduct the burns, the benefit is not substantial (approximately 6 km; Figure D.4). Instead, it is much more advantageous to conduct the burns roughly one-half of an orbital revolution apart (approximately 30 km; Figure D.5). In conclusion, keeping the burns one-half revolution apart is more important than where the burns occur in the orbit.

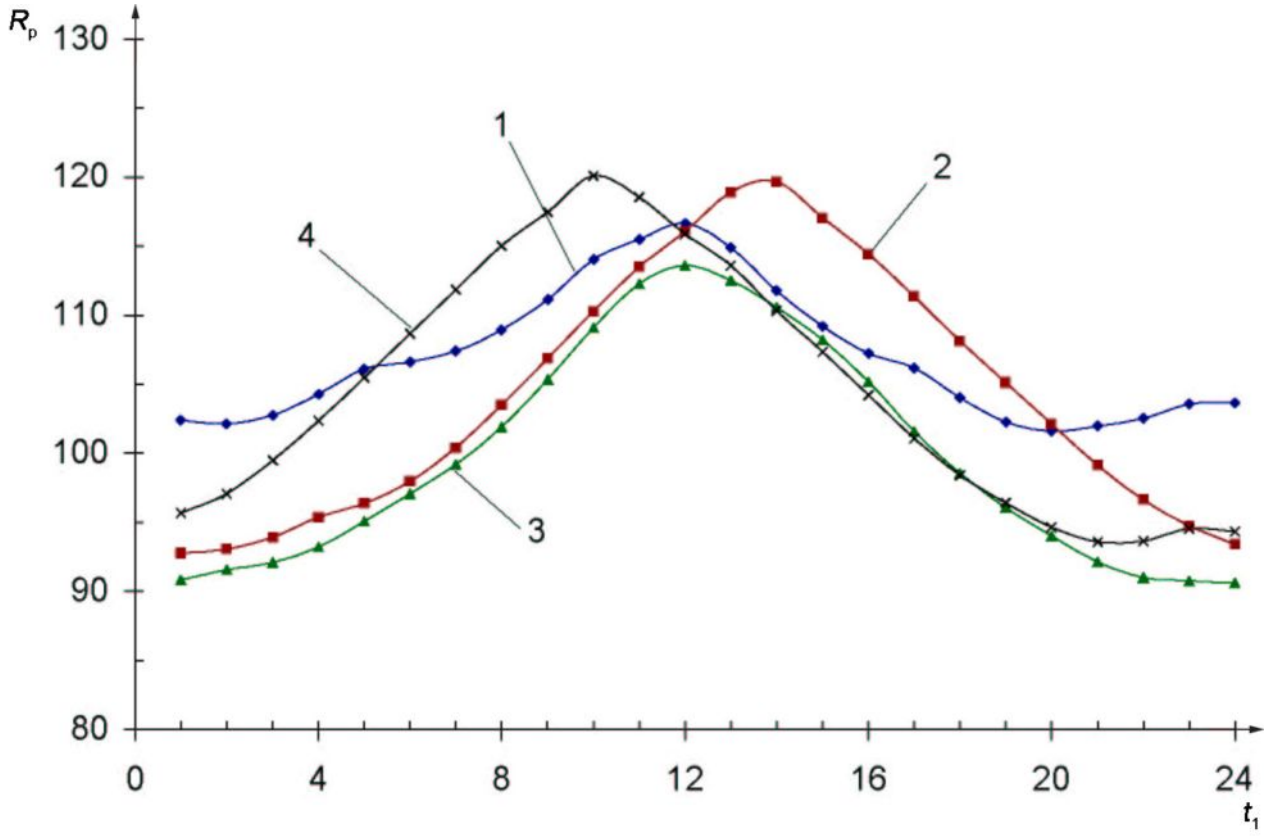


**Key**

$R_p$ minimum perigee altitude over 100 years, in km
$t_1$ hours past perigee for first burn in the pair
1 0 h
2 5 h
3 12 h
4 20 h

**Figure D.5 — Individual sample cases from Figure D.4**

The effectiveness of the proposed eccentric burn strategy is shown in Figure D.6 as a function of cumulative $\Delta V$. Three burn profiles are given. The first is the proposed eccentricity control strategy in which an initial 0,5 m/s burn is applied near perigee, followed by a smaller 0,25 m/s burn 24 h later to establish the orbit near the target $e$ and $\omega$. This is then followed by 0,5 m/s burn pairs about 36 h apart conducted in such a way as to keep $e$ and $\omega$ to within 0,000 14 and 10° of optimal, respectively. The circularization strategy assumes the original orbit ($e = 0{,}000\,317$ and $\omega = 353°$) and conducts burns of 0,5 m/s at apogee and perigee. In this manner, the original $\omega$ is maintained close to 353°. The proposed eccentricity strategy results in a much more favourable clearance of the GEO belt than simple apogee-perigee burns. The worst profile is the apogee-perigee burn pairing coupled with an initial argument of perigee of 200°. This situation should be avoided at all costs.

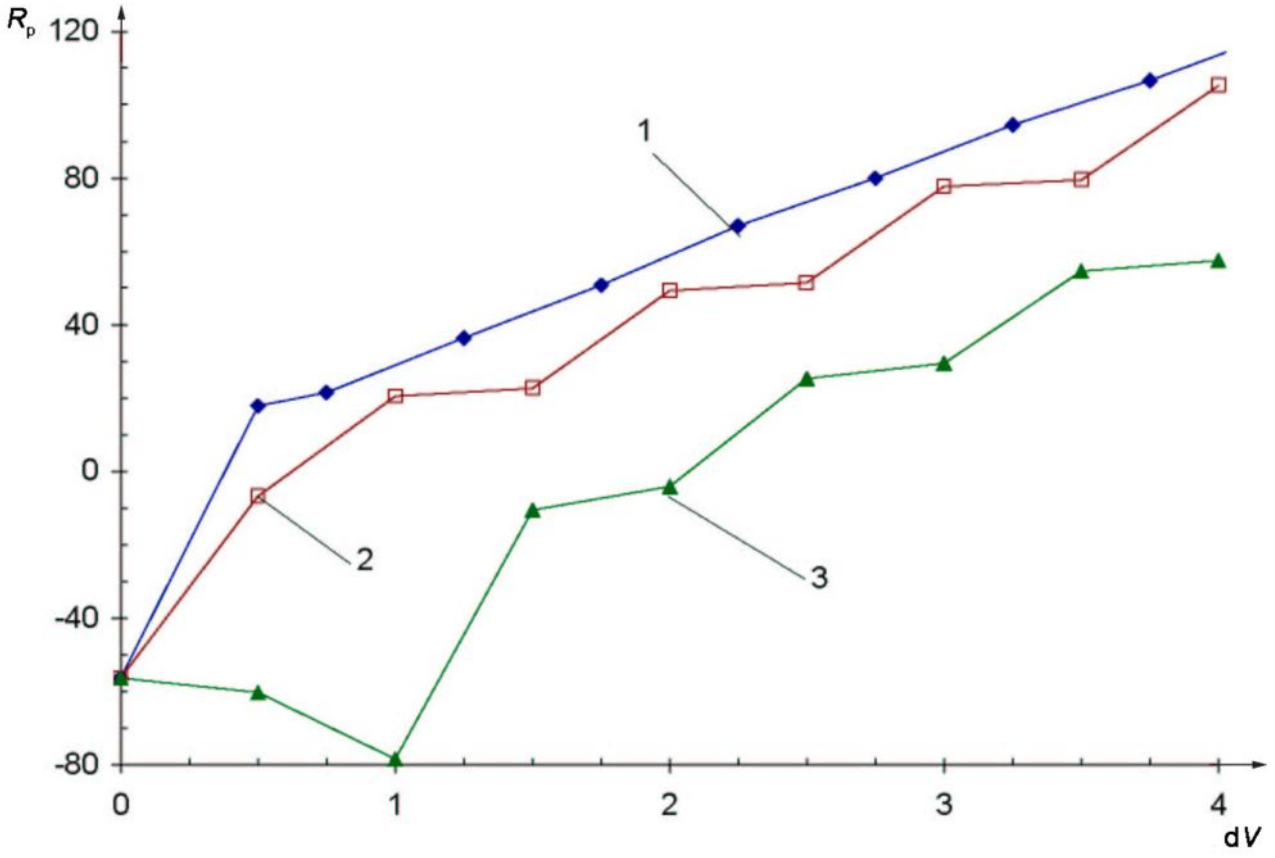


**Key**

$R_p$ minimum perigee altitude over 100 years, in km
d$V$ cumulative $\Delta V$, in m/sec
1 eccentric profile
2 circularized profile
3 worst profile

**Figure D.6 — Effectiveness of proposed strategy for sample GEO case**

In conclusion, targeting the optimal eccentricity and argument of perigee during the disposal manoeuvres can make a significant improvement in the 100-year clearance of the GEO belt as opposed to simply burning in the usual apogee-perigee manner. However, the results derived from this study imply that while the sun-pointing strategy is close to the true optimal argument of perigee and eccentricity, lunar perturbations will cause the optimal values to be slightly different than the pure sun-pointing values. Therefore, the true optimal value should be determined on a case-by-case basis.

# Annex E
(informative)

# Discussion of conditional probability

## E.1 General

The requirement given in 7.2 that "a spacecraft shall be designed such that the joint probability of having sufficient energy (propellant) remaining to achieve the final disposal orbit and successfully executing commands to deplete energy sources equals or exceeds 0,9 at the time disposal is executed" represents a typical and consistent approach to managing the multiphased mission from a probability point of view.

Assuming the orbital scenario is constituted by the two main phases

— nominal mission, $M$, and

— disposal, $D$,

the conditional probability theorem allows us to state

$$P(M \cap D) = P(M) \times P(D/M) \tag{E.1}$$

It follows that

$$P(D/M) = \frac{P(M \cap D)}{P(M)} \tag{E.2}$$

Therefore, the probability, $P(D/M)$, of successfully performing the end-of-mission disposal once the nominal mission has been completed may be estimated on the basis of the following:

a) $P(M)$: mission success probability (normally evaluated in the frame of the dependability program to verify the compliance of the developed design with regard to the applicable mission reliability requirement), and

b) $P(M \cap D)$: probability of correctly performing both mission and disposal phases [this is generally an extension of the $P(M)$ model].

Cases 1 to 3 below are presented to clarify the application of Equation (E.2).

## E.2 Case 1

The end-of-mission disposal is performed making use of "all" subsystems involved in the nominal mission (mechanical, electrical, propellant, propellant measurement uncertainties, etc.), as illustrated in the Venn diagram shown in Figure E.1.

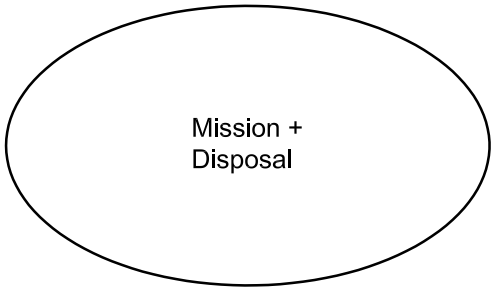


**Figure E.1 — All subsystems involved in the nominal mission required for disposal**

In this way, the reliability model defined for the nominal mission (0; $T_{\text{mission}}$) is extended to cover both phases (0; $T_{\text{mission}} + T_{\text{disposal}}$).

$$P(D/M) = \frac{R_{\text{system}}(T_{\text{mission}} + T_{\text{disposal}})}{R_{\text{system}}(T_{\text{mission}})} P_{\text{propellant}} \tag{E.3}$$

where

$P_{\text{propellant}}$ is the probability of there being sufficient propellant to perform a successful transfer to and injection into the final disposal orbit;

$R_{\text{system}}$ is the reliability of all the systems used for normal operations.

## E.3 Case 2

The end-of-mission disposal is performed making use of “some” subsystems involved in the nominal mission, as illustrated in the Venn diagram shown in Figure E.2.

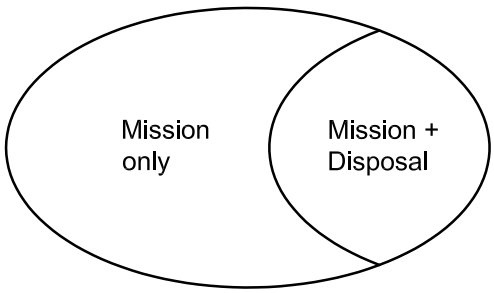


**Figure E.2 — Some subsystems involved in the nominal mission are used for disposal**

In this case, the function $R'_{\text{system}}(t)$ includes the reliability of the subsystems used for disposal estimated over the interval (0; $T_{\text{mission}} + T_{\text{disposal}}$). For the subsystems not used for disposal, the interval (0; $T_{\text{mission}}$) is considered. For all subsystems, the reliability models defined for mission success may be used, even if with different time durations.

The reliability function $R_{\text{system}}(t)$ refers to the nominal mission (as presented in Case 1).

$$P(D/M) = \frac{R'_{\text{system}}(T_{\text{mission}} + T_{\text{disposal}})}{R_{\text{system}}(T_{\text{mission}})} P_{\text{propellant}} \tag{E.4}$$

## E.4 Case 3

The end-of-mission disposal is performed making use of "dedicated" equipment and some subsystems involved in the nominal mission, as illustrated in the Venn diagram shown in Figure E.3.

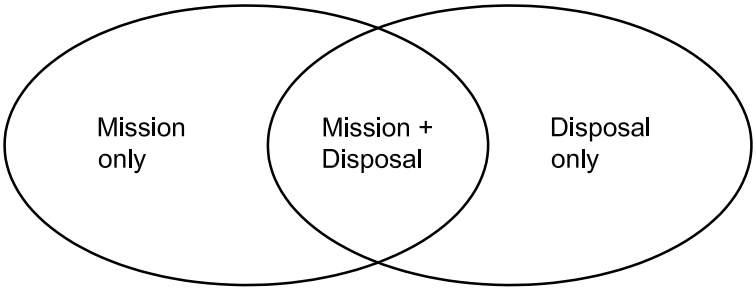


**Figure E.3 — Disposal requires some systems used for normal operations plus some systems specifically used for disposal only**

In this extension of Case 2, the $R''_{\text{system}}(t)$ function includes the contribution of the equipment for disposal: considered in active or passive mode (as applicable) in the interval (0; $T_{\text{mission}}$) and in active mode in the interval ($T_{\text{mission}}$; $T_{\text{mission}} + T_{\text{disposal}}$).

The reliability function, $R_{\text{system}}(t)$, refers to the nominal mission (as presented in Case 1).

$$P(D/M) = \frac{R''_{\text{system}}(T_{\text{mission}} + T_{\text{disposal}})}{R_{\text{system}}(T_{\text{mission}})} P_{\text{propellant}} \tag{E.5}$$

Several cases may be described. The cases presented in this annex are provided to clarify the approach taken in this International Standard.

# Bibliography

[1] ISO 16127[4)], *Space systems — End of life passivation of unmanned spacecraft*

[2] ISO 23339[4)], *Space systems — Unmanned spacecraft — Requirements for estimating the mass of remaining usable propellant*

4) Under preparation.

**ICS 49.140**

Price based on 53 pages

*This page deliberately left blank*

# British Standards Institution (BSI)

BSI is the independent national body responsible for preparing British Standards and other standards-related publications, information and services.
It presents the UK view on standards in Europe and at the international level.

It is incorporated by Royal Charter.

## Revisions

British Standards are updated by amendment or revision. Users of British Standards should make sure that they possess the latest amendments or editions.

It is the constant aim of BSI to improve the quality of our products and services. We would be grateful if anyone finding an inaccuracy or ambiguity while using this British Standard would inform the Secretary of the technical committee responsible, the identity of which can be found on the inside front cover.

**Tel: +44 (0)20 8996 9001 Fax: +44 (0)20 8996 7001**

BSI offers Members an individual updating service called PLUS which ensures that subscribers automatically receive the latest editions of standards.

**Tel: +44 (0)20 8996 7669 Fax: +44 (0)20 8996 7001**
**Email: plus@bsigroup.com**

## Buying standards

You may buy PDF and hard copy versions of standards directly using a credit card from the BSI Shop on the website **www.bsigroup.com/shop.** In addition all orders for BSI, international and foreign standards publications can be addressed to BSI Customer Services.

**Tel: +44 (0)20 8996 9001 Fax: +44 (0)20 8996 7001**
**Email: orders@bsigroup.com**

In response to orders for international standards, it is BSI policy to supply the BSI implementation of those that have been published as British Standards, unless otherwise requested.

## Information on standards

BSI provides a wide range of information on national, European and international standards through its Knowledge Centre.

**Tel: +44 (0)20 8996 7004 Fax: +44 (0)20 8996 7005**
**Email: knowledgecentre@bsigroup.com**

Various BSI electronic information services are also available which give details on all its products and services.

**Tel: +44 (0)20 8996 7111 Fax: +44 (0)20 8996 7048**
**Email: info@bsigroup.com**

BSI Subscribing Members are kept up to date with standards developments and receive substantial discounts on the purchase price of standards. For details of these and other benefits contact Membership Administration.

**Tel: +44 (0)20 8996 7002 Fax: +44 (0)20 8996 7001**
**Email: membership@bsigroup.com**

Information regarding online access to British Standards via British Standards Online can be found at **www.bsigroup.com/BSOL**

Further information about BSI is available on the BSI website at **www.bsigroup.com/standards**

## Copyright



**Tel: +44 (0)20 8996 7070**
**Email: copyright@bsigroup.com**

**BSI Group Headquarters**

389 Chiswick High Road London W4 4AL UK

Tel +44 (0)20 8996 9001
Fax +44 (0)20 8996 7001
www.bsigroup.com/standards

*raising standards worldwide*™